NASA TECHNICAL TRANSLATION NASA TT F-16184

STUDIES RELATIVE TO THE INDUCTION PRESSURIZED TRANSONIC WIND TUNNEL B. START-UP: SETTING-UP TIME

C. Quemard, A. Mignosi and A. Seraudie

Translation of "Etudes relatives a une soufflerie transsonique pressurisee a induction. B) Mise en marche; temps d'etablissement," Technical Note No. 6/5006, Department d'Etudes et de Recherches en Aerothermodynamique, Centre d'Etudes et de Recherches de Toulouse, O.N.E.R.A., July 1974, pp. 1-40

NATIONAL AERONAUTICS AND SPACE ADMINISTRATION
WASHINGTON, D.C. 20546 MARCH 1975

STANDARD TITLE PAGE

1. Report No. NASA TT F-16184	2. Government Accession No.	3. Recipient's Catalog No.
4. Title and Subtitle STUDIES RELATIVE TO THE INDUCTION PRESSURIZED TRANSONIC WIND TUNNEL B. START-UP: SETTING-UP TIME		5. Report Date March 1975 6. Performing Organization Code
7. Author(s) C. Quemarde, A. Mignosi and A. Seraudie		8. Performing Organization Report No. 10. Work Unit No.
9. Performing Organization Name and Address Leo Kanner Associates Redwood City, California 94063		11. Contract or Grant No. NASw-2481 13. Type of Report and Period Covered
12. Sponsoring Agency Name and Address National Aeronautics and Space Administration, Washington, D.C. 20546		14. Sponsoring Agency Code

15. Supplementary Notes

Translation of "Etudes relatives une soufflerie transsonique pressurisee a induction. B) Mise en marche; temps d'etablissement," Technical Note No. 6/5006, Department d'Etudes et de Recherches en Aerothermodynamique, Centre d'Etudes et de Recherches de Toulouse, O.N.E.R.A., July 1974, pp. 1-40

16. Abstract

The problem of starting an induction wind tunnel with return circuit is discussed. The basic equations governing start-up are given, and the principal experiments conducted with the T'2 wind tunnel with peripheral injection are shown. Finally the results of experiments abd of the computation are discussed and a comparison of experiment and computation is made.

17. Key Words (Selected by Author(s))	18. Distribution Statement
	Unclassified-Unlimited

19. Security Classif. (of this report)	20. Security Classif. (of this page)	21. No. of Pages	22. Price
Unclassified	Unclassified	43	

TABLE OF CONTENT /1

/2

ANNOTATIONS

$\omega(x)$ - Surface of the x abscissa
p - Density
x - Abscissa of the point
t - Time
p - Static Pressure
T - Temperature
s - Specific Entropy
M - Mach Number
P_i - Stagnation Pressure
T_i - Stagnation Temperature
h_i - Stagnation Enthalpy
a - Speed of Sound
u - Velocity of Flow
K - Length of
m' - Injected (or Discharged) Air Flow per Unit of Length
j' - Dynalpy of Injected (or Discharged) Air per Unit of Length
f' - Force of Friction per Unit of Length
q' - Injected (or Discharged) Heat Transfer Rate per Unit of Length
q - Flow

INDICES

w - Variable Taken at the Wall
j - Injection
e - Discharge
v - Nozzle Throat
m - Mixer
1 - Upstream of Injector
2 - Downstream of Injector
o - Initial Starting Conditions
s - Steady State
$(-)$ - Reduced Variables

INTRODUCTION

The problem of starting an induction wind tunnel with return circuit is important in order to minimize the energy lost during this transient phase. While the starting time is relatively short, of the order of a few tenths of a second in a small-sized wind tunnel (about ten meters in length), it becomes a basic element in the case of a wind tunnel of about 100 meters in length, where the gust time ranges from 10 to 30 seconds. In the latter case, the starting time is of the order of several seconds and may impair the performance of such a project from the energy standpoint.

In a first part, we will present the basic equations, which govern starting in a first approximation. We will then show the principal experiments conducted on the T'_2 with peripheral injection and then with corner injection. Finally, we will show the results of the computation established by Mr. Capelier, which solves the basic equations and checks the experiments quite satisfactorily.

I. ANALYSIS OF STARTING

I.1. Presentation of the T'_2 Wind tunnel:

We used three types of wind tunnels (figure 1):

A — Mach $M_j = 1$ peripheral injection wind tunnel;

B — Mach $M_j = 1$ corner injection wind tunnel;

C — Mach $M_j = 1.6$ corner injection wind tunnel.

All of these wind tunnels comprise a settling chamber, a collector, a nozzle throat, a discharge and injection device, a diffuser followed by a return section.

We will take the plane of the injectors as the arbitrary origin in order to write the starting equations.

From the starting equations we have retained:

— The length of the circuit;

— The area rule $\omega(x)$;

---

* Numbers in the margin indicate pagination in the foreign text

— The geometry of the injector: position, surface ratio;

— The injection conditions

(Mach number, stagnation pressure, stagnation temperature of the injector).

— Pressure drops (boundary layers, screens, base drags);

— The outlet valve opening pattern (possible shift with respect to intake). /5

The characteristic starting times are:

(H) Time in which injector reaches maximum flow;

L/q_o Time in which a sound wave makes a complete turn of the circuit.

L/u_{mean} Time in which the fluid makes a complete turn of the circuit.

I.2. Starting Equations

The theoretical problem was solved by Mr. Carriere (The Injector Driven Tunnel), the basic equations express the conservation of mass, dynalpy, energy:

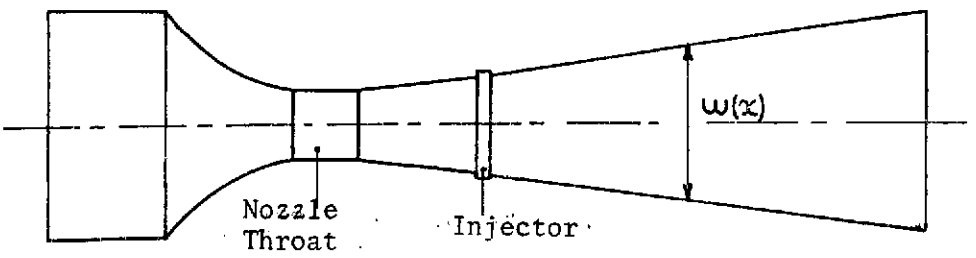

$$(1) \quad \frac{\partial}{\partial t}(\rho\omega) + \frac{\partial}{\partial x}(\rho\omega u) = m'$$

$$(2) \quad \frac{\partial}{\partial t}(\rho\omega u) + \frac{\partial}{\partial x}(p + \rho u^2) = p_w \frac{\partial \omega}{\partial x} + j' - f'$$

$$(3) \quad \frac{\partial}{\partial t}(\rho\omega h_i) + \frac{\partial}{\partial x}(\rho\omega u h_i) = \frac{\partial}{\partial t}(p\omega) + q'$$

where: m' = Injected (or discharged) air flow per unit of length;
j' = Injected (or discharged) air dynalpy per unit of length;
f' = Friction force per unit of length;
q' = Injected (or discharged) heat transfer rate per unit of length;
Pw = Pressure at the wall

I.3. Numerical Treatment /6

In order to treat these equations numerically, Mr. Capelier used a schematization of the circuit treating the injector as a discontinuity. The circuit was opened at the level of the injector.

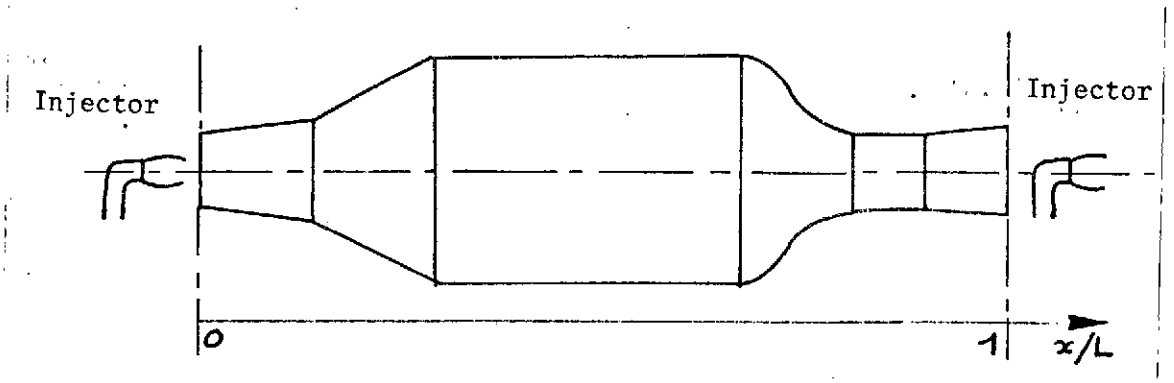

When equation (3) brings in h_i it can be transformed by using entropy s of the flow.

$$(3) - (1)h_i \qquad \frac{dh_i}{dt} = \frac{1}{\rho}\frac{\partial p}{\partial t} + \frac{q' - m'h_i}{\rho}$$

If we use the thermodynamic relation

$$dh_i = T\,ds + \frac{dp}{\rho} + u\,du$$

we have:

$$(3)' \qquad \frac{ds}{dt} = -\frac{u}{\rho T}\left(j' - f' - m'u\right) + \frac{q' - m'h_i}{\rho T}$$

The program thus solves the system distinguishing two parts

$$\frac{\partial}{\partial t}(\rho\omega) + \frac{\partial}{\partial x}(\rho\omega u) = m'$$

$$\frac{\partial}{\partial t}(\rho\omega u) + \frac{\partial}{\partial x}\left((p + \rho u^2)\omega\right) = p\frac{d\omega}{dx} + j' - f'$$

$$\frac{\partial s}{\partial t} + u\frac{\partial s}{\partial x} = -\frac{u}{\rho T}\left(j' - f' - m'u\right) + \frac{q' - m'h_i}{\rho T}$$

(a) Outside the Injector:

The term $q' - m'h_i$ can then be assumed to be zero. It is then necessary to outline the discharge calculating j' as a function of time and of x, two parameters, m' and j', thus remain.

If discharge is made at a velocity u_e on a surface ω_e, at a pressure P_e ... etc.

$$j' = \frac{\partial j}{\partial x} = \frac{\partial}{\partial x}\left(P_e\left(1+\gamma M_e^2\right)\omega_e - P_{we}\right)$$ /7

Two parameters are included in this expression, ω_e and M_e, or, if desired, M_e and $q_e = \rho_e \omega_e u_e$, since rate of flow is given by

$$q_e = \frac{\lambda(\gamma)\,\omega_e P_{ie}}{\sqrt{T_{i_0}}\,\Sigma(M_e)}$$

In the case of the computations presented here, we made the supplementary hypothesis that the outlet velocity of discharge is equal to that of flow; that leaves only one parameter, q_e.

$$j = \left(p + \rho u^2\right)\omega_e - p\omega_e = \rho u^2 \omega_e = q_e u$$

$$j' = m'u$$

The equations are then written

$$\frac{\partial(\rho\omega)}{\partial t} + \frac{\partial(\rho\omega u)}{\partial x} = m'$$

$$\frac{\partial}{\partial t}(\rho\omega u) + \frac{\partial}{\partial x}\left(\left(p+\rho u^2\right)\omega\right) = p\frac{d\omega}{dx} + m'u - f'$$

$$\frac{\partial s}{\partial t} + u\frac{\partial s}{\partial x} = -\frac{u}{\rho T} f'$$

m' = the flow discharged per unit of length (a function of x and of t).

(b) At the Level of the Injector

The system written at the level of the injector becomes:

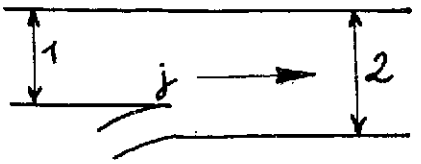

$$\rho_1 u_1 \omega_1 + \rho_j u_j \omega_j = \rho_2 u_2 \omega_2$$

$$(p_1 + \rho_1 u_1^2)\omega_1 + (p_j + \rho_j u_j^2)\omega_j = (p_2 + \rho_2 u_2^2)\omega_2$$

$$\left(h_1 + \frac{u_1^2}{2}\right) q_1 + \left(h_j + \frac{u_j^2}{2}\right) q_j = \left(h_2 + \frac{u_2^2}{2}\right) q_2$$

The solution program uses a discrimination following the MacCormack scheme shown in the appendix. The results of the computation are discussed following the presentation of the experimental results. We have, however, shown (figure 2) a typical case of starting computation to show the main phenomena that appear at the time of start-up: progressive increase in velocity, stagnation or entropy temperature wave. /8

II. FIRST EXPERIMENTAL TESTS

II.1. Experimental Study with Peripheral Injection (M_j = 1)

(a) Rig

We used a schematized rig (figure 3). The injection system operates by turning a three-way valve that first discharges the flow to the outside. Discharge takes place after the second corner and can be opened very rapidly (time comparable to the increase of Pij).

Pressures Piv, Psv, Pij were measured by means of pick-ups and recorded graphically, the Mach number is obtained from Psv/Piv.

(b) Types of Tests Conducted

A. Open exhaust, filling of the wind tunnel and start-up by

the injection of air;

B. Closed exhaust, filling of the wind tunnel and start-up by the injection of air, opening of the exit at the time when pressure Piv reaches its operating level;

C. Closed exit, prior charging of the wind tunnel by means of and attached system, start-up by air injection with simultaneous opening of the exhaust.

II.2. Results (figure 3)

In the three cases considered, the Pij follows the same curve as a function of time, rise time (H) being of the order of 15/100 sec.

In Case A, pressure Piv attains its operating value asymptotically in a period of time of about 10 sec.

In Case B, since the exit is closed, Piv increases rapidly: setting-up time, 1 sec. If rise time Pij and the masses of high-velocity air are neglected, a time corresponding to the mass of air to be injected necessary to raise the pressure from 1 bar (atmospheric pressure) to Piv = 1.7 bar is obtained. In the case of the experiment (wind-tunnel capacity 0.9 m^3)

Initial mass	1.2 x 0.9	= 1.08 kg
Injected mass	0.85 x 1	= 0.85 kg
Final mass		1.93 kg

This corresponds more of less to a Piv of 1.7 bar if the temperature is 273°K. It is likely that temperature Tiv will increase sharply at the time of charging. /9

In case C, since the wind tunnel is pressurized, the Mach setting-up time corresponds to start-up and friction inertia. It is of the order of 4/10 sec. The initial slope is not so steep as in the case of A and B, since the initial mass to be driven is greater.

III. PRECHARGED TESTS WITH A TWO-VANE CORNER $M_j = 1.6$

III.1. Circuit Diagram

(a) We have a circuit 10.7 meters long. Injection takes place through a two-vane corner whose outlet Mach number is $M_j = 1.6$. Each vane carries 4 nozzles at the trailing edge, the start of injection is obtained by turning the three-way valve and directing the injection flow from an outlet in the atmosphere to the flexible feed tubes of the tunnel.

We have the possibility of injecting air at different temperatures thanks to a heater.

The capacity between the three-way valve and the vanes is at least 2.6 liters, but it can be increased by the addition of flexible tubes.

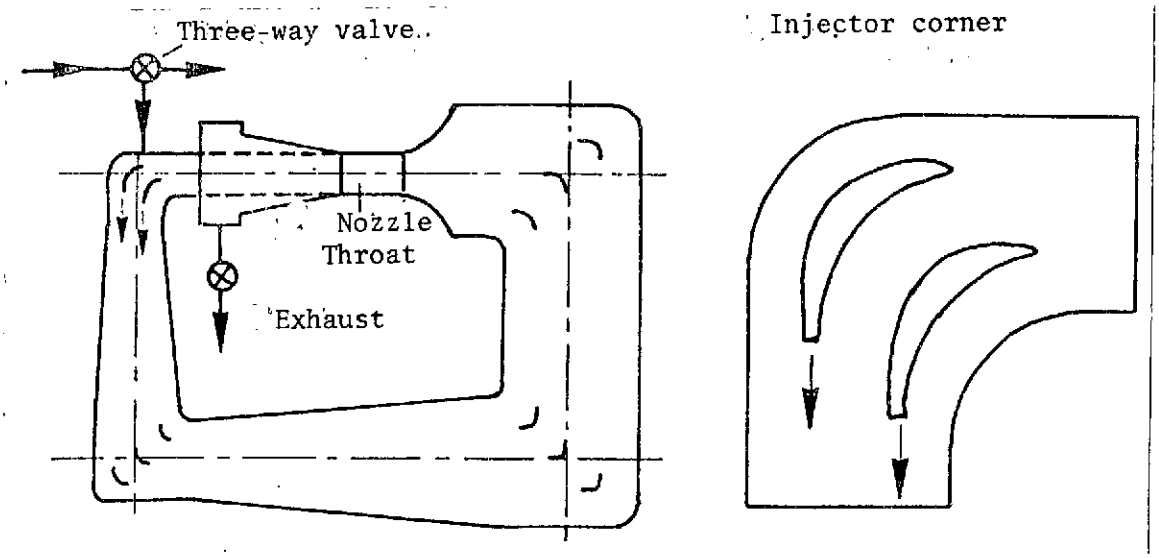

(b) The exit is controlled by a fast-opening valve whose shift in time with respect to the input flow is adjustable.

(c) The cross-sectional pattern of the wind tunnel, as well as the pressure-drop curve corresponding to the nozzle throat Mach number of 0.8 are given (figure 10).

III.2. Measurements Made

(a) Pressure Measurements

We developed a Pitot tube whose reponse time is the shortest possible. It comprises a Pi intake and a Ps intake through four orifices. This Pitot tube was placed in the nozzle throat. ✓10

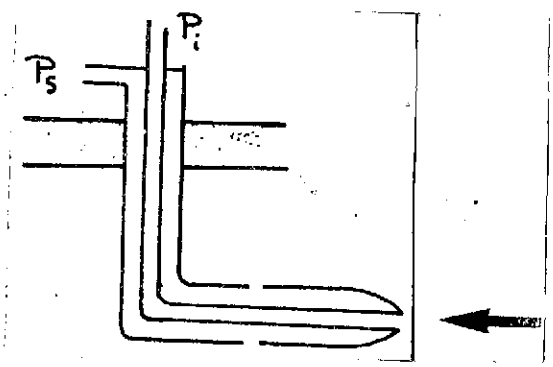

Pressure measurement is made by means of BAUDOIN pick-up operating differentially, the maximum value of Δp being of the order of 50 mb. Each pressure Ps and Pi is opposed to a fixed pressure maintained in a reservoir, the measurement of Ps is triggered by an electrovalve, thus making it unnecessary to have a very substantial suppression on the Ps pick-up.

At rest, electrovalve Ev2 connects points 2, 3, 4, inlet 1 being closed. When the measurement of Psv is triggered, electrovalve Ev2 connects 1 and 4 at the same time as 2 and 3, pick-up Cs thus measures Psv-PsR at this moment. In the experiments conducted, the Piv reservoir was always charged up to the wind tunnel charging pressure. The Psv reservoir was charged to a pressure in the vicinity of the value of the Psv in steady operation.

We tested the Pitot probe with respect to the response of the system at a step of Δp. If the diaphragm is

caused to break so as to obtain a pressure step, both pick-ups Ci and Cs respond appreciably as of the first orders. The passband corresponding to this response is of the order of 300 Hz. Recording of these measurements is made on paper capable of fast unwinding. /11

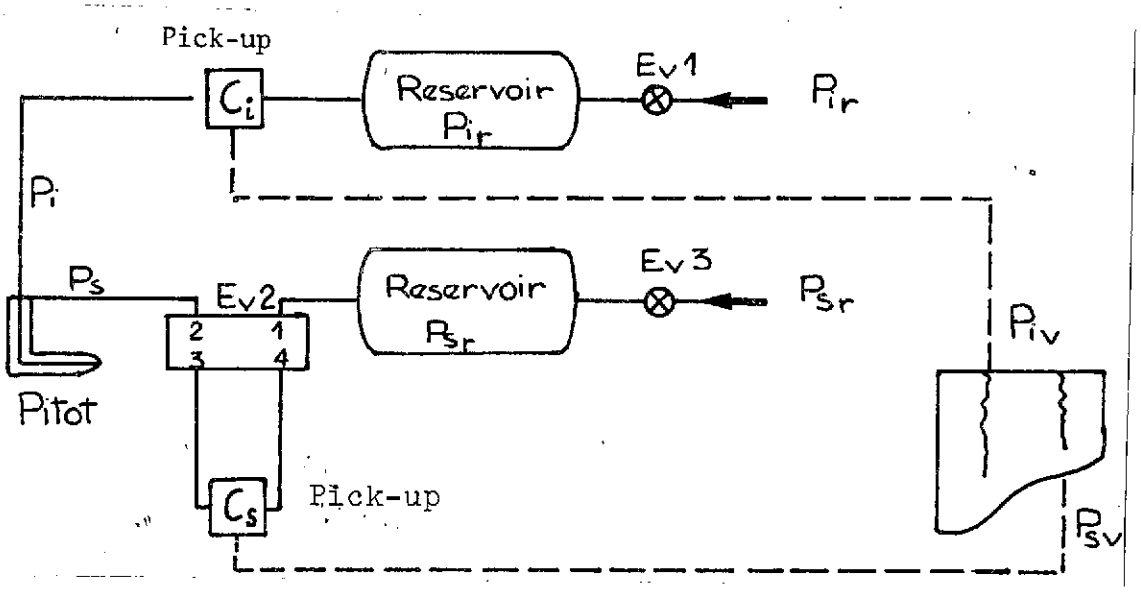

(b) Measurement of Stagnation Temperatures

Temperatures are measured by means of "chromel-alumel" thermocouples in which the wire diameter is less than one tenth of a millimeter. Response time is a function of the velocity of flow and it is difficult to calculate, but it may be said, however, that it is sufficient to observe a jump in temperature in a time of less than 5/100 of a second.

(c) Location of the Different Probes

We showed (figure 4) the position and the names of the different pressure and temperature probes. The main ones are:

1. Pressure

Piv Nozzle throat stagnation pressure

Psv Nozzle throat static pressure

Pij Injection stagnation pressure

2. Temperature

Tiv Stagnation temperature in the collector

Tim Stagnation temperature at the end of the second diffuser

Tij Stagnation temperature at the vane

III.3. Description of a Precharged System Starting

In order to start the T'_2 wind tunnel, the system is first charged to a pressure P_d (starting pressure) in the neighborhood of the nozzle throat generator pressure Piv, the inlet and outlet valves are then opened with each of the opening patterns virtually identical in each test, but shifted in time with respect to each other.

We caused a certain number of starting conditions to vary in an attempt to determine the effect of different parameters.

-- The injection temperature can be adjusted to different values for the steady state, but we do not control the Tij pattern during the first tenths of a second (filling of the cavities between the three-way valve and the T'_2 wind tunnel).

-- Pressure drops in the wind tunnel were modified by the indroduction of screens creating supplementary pressure drops in any part whatsoever of the system.

-- The time shift of the intake and outlet openings can

be either positive or negative.

-- The rise time of Pij could be modified by increasing the charging capacities downstream of the three-way valve. /12

III.4. Results of the Experiments

(a) Characteristics Common to the Different Experiments

-- The shape of the rise curve of Pij is exponential, the rise time being of the order of 1 to 2 tenths of a second.

-- The injection temperature involves a "peak" whose duration is of the same order as the rise time of Pij.

-- The nozzle throat Mach number in the steady state is of the order of $M_v \simeq 0.8$.

(b) Development of the Temperature Along the Circuit: Fig. 5.

We measured the temperature at different points of the circuit by means of thermocouples.

The creation of a sinusoidal-shaped temperature wave is observed behind the injectors. Temperature rises, then drops. This "entropy pocket" propagates in the circuit at the speed of flow, or about 20 m/sec with progressive attenuation. A qualitative value must be attached to this series of curves, since the conditions are not the same for each thermocouple.

The rise in temperature at the nozzle throat can be explained by a compression phenomenon. The pressure drops in

the settling chamber and the return section screens cause a recompression of the wind-tunnel air which becomes greater as we move up the circuit.

(c) Effect of a Supplementary Pressure Drop: Figure 6.

In order to show the importance of pressure drops in the return section and the effect thereof, we introduced a supplementary pressure drop at the outlet of the third corner between Ti_3 and Ti_4. If two tests, with or without pressure drop, are compared, the beginning of an identical curve for $t < 0.25$ sec at Tiv, then a temperature "hump" linked to the air, located between the injectors and the pressure drop introduced, where it is compressed on starting will be observed.

(d) Effect of the Shift of Inlet-Outlet Openings: Figure 7

A substantial effect is observed during the first tenth of a second. If the outlet is opened very late (case A), temperature rises abruptly, and so does pressure Piv. If it is opened early (case B), both temperature and pressure drop.

A slight rise in temperature and then a sharp drop, probably due to the "entropy pocket" phenomenon, is then observed. The duration of a complete passage through the circuit is 4/10 of a second. The shape of the curve with a damping of the order of 2 to 3 for each complete passage through the circuit is then encountered periodically. /13

(e) Influence of Injection Temperature: Figure 8

We injected air using a heater in order to increase the Tij curve by 16°C.

The hot air acts on the Tiv curves at the level of the temperature rise and accentuates the temperature "hump."

There is then a deviation in the temperature, which only rises due to the progressive heating of the system.

(f) Presentation of a typical test with a Throat Downstream of the Nozzle Throat.

We presented a test conducted with a T'_2 with a generator pressure of the order of 2 bars, the injection pressure being set-up at 15/100 sec. The injection temperature was measured at the injector vane itself and shows a "peak" of the order of 8°C for a time of the order of one tenth of a second.

The flow characteristics are:

-- A Piv setting-up time of the order of 3/10 of a second after the sharp drop due to the opening of the outlet valve and to start-up.

-- A setting-up time of the Mach number Mv of the order of 3/10 of a second.

-- A temperature variation in the nozzle throat whose curve is plotted at the bottom of the figure. An initial drop in temperature due to starting and to the opening of the outlet is observed. Then a progressive rise in temperature followed at the end of 4/10 of a second by a drop of the order of 1°C.

IV. RESULTS OF THE STARTING COMPUTATION AND COMPARISONS WITH EXPERIMENTS

IV.1. Choice of Computation Parameters

(a) For the injector we selected a Pij rise pattern as a function of time satisfying the conditions for t = 0, Pij = Po; for t → ∞, Pij = C^{te}

either exponential $P_{ij}/P_o = 1 + A\left(1 - e^{-\alpha t}\right)$

or parabolic
$$\begin{cases} P_{ij}/P_o = 1 + A\left(1 - \left(\frac{t-\tau}{\tau}\right)^2\right) & \text{for } t < \tau \\ P_{ij}/P_o = 1 + A & \text{for } t \geq \tau \end{cases}$$

We took a rise pattern of Mach Mj /14

We selected an injection temperature pattern Tij as a function of time.

(b) For discharge, we selected a discharged flow pattern m' of the parabolic type

$$\begin{cases} m' = B\left(1 - \left(\frac{t-\tau_e}{\tau_e}\right)^2\right) & \text{for } t < \tau_e \\ m' = B & \text{for } t \geq \tau_e \end{cases}$$

We must satisfy the conditions m' = 0 for t = 0, and m' = injected flow for t → ∞.

(c) For the drops in the system, $f' = \frac{\partial f}{\partial x}$ must be given at each point and at every moment.

For the steady state we selected a Pis (x) curve close to that of the experiment, from which f'_s was derived by:

$$f'_s = \omega P_s \frac{dP_{is}}{dx} \frac{1}{P_{is}}$$ (See appendix)

In order to take into account the variations in pressure drops at the time of starting, we adopted a drop pattern proportional to the square of the velocity at the point involved, that is, for f'

$$f' = f'_s \frac{P}{P_s} \left(\frac{u}{u_s}\right)^2$$

(d) An area rule S(x) must also be given all alone the circuit; we flattened the experimental curve to avoid computation oscillations, see figure 10.

IV.2. Generalities Prior to the Analysis of Results

In order to present the numerical results obtained as a function of the computation parameters, we will have to adopt a dual point of view. If X is a variable depending on x and t we may:

-- Consider the variation of X along the circuit at a given moment: $X = X(x, t_o)$.

-- Take a point in the circuit and plot the variation of X as a function of time: $X = X(x_o, t)$.

A dual purpose was assigned to this computation:

1. To determine that virtually the same results are obtained: increase of the Mach number, temperature variations pressure variations, etc., as in T'_2, when inlet parameters close to the experimental ones are taken.

2. To determine the effect of each parameter, in order to minimize the energy or injected air mass lost in starting; /15
certain criteria must then determine from what time the velocity in the wind tunnel can be deemed sufficiently stable: a nozzle-throat Mach number that does not vary beyond ε from the assigned value.

It is desirable for Tiv not to vary more than ε% from a value, etc.

IV.3. Experiment-Computation Comparison

We have represented (figure 11) the mathematical expressions taken for the different computation parameters, and the values that the experiment furnished in a test at Mv = 0.8 without a throat.

Figure 12 compares the development of Piv measured by the previously described double Pitot tube, as well as the increase in the Mach number. We have represented the variation in stagnation pressure at the point $\bar{x} = 0.9$ corresponding to the beginning of the nozzle throat.

The stagnation pressure measured by the probe consists initially of a sharp drop due in all likelihood to the outlet opening pattern; then, at the end of a time of the order of 1/10 of a second, this experimental curve is interposed between the other two. One can not say that it is the acutal mean Pi at the level of the nozzle throat, the probe only measures the pressure at the center of the flow.

While a good initial agreement is observed in the case of the rise pattern of the nozzle-throat Mach number, the computation then deviates from the experiment. The three-dimensional effects are important at the level of the nozzle throat, where the boundary layers cause an increase in the Mach number at the end of the nozzle throat.

The Pitot tube that measures pressures also has an effect which is not taken into account in the computation. The presence of a throat in the previously presented experiments shows that the rise time of the nozzle throat Mach number can be reduced to 2/10 of a second.

We encounter this effect through computation by imposing

a state of equilibrium at $M_v \simeq 1$ and considering that when M_v reaches 0.8, a fictitious throat comes into play causing the throat Mach number to remain at that value.

Figure 13 compares temperature developments between two points in the system. We have represented the temperature variations at the level of the second T'_2 corner, or $\bar{x} = 0.2$, and the temperature at the level of the collector, or $\bar{x} = 0.8$, point where the measurement was made.

The general shape of the experimental curves is obtained by computation. The substantial deviation between the experimental curves and computation are due in part to the fact that we do not take into account heat transfers between the fluid and the wind tunnel. There are also three-dimensional effects that must favor the disapperance of the temperature "peaks."

IV.4. Effect of the Different Parameters /16

(a) Effect of Pressure Drops

We compared two cases of starting in which the parameters were identical (rise pattern of q_j and of $j(t)$, also exhaust, etc.) but where the pressure drop of the circuit was distributed differently, see figure 14.

There is no pressure drop in the return section in case B, and the pressure drop in case A is of the order of 2%.

Very little difference is observed between the two cases when the nozzle-throat Mach number is setup; conversely, there is a very decided difference when we consider the development of stagnation temperatures in the collector.

In case B, the temperature remains constant from $\bar{t}$ = 6 to $\bar{t}$ = 12: the mass of air situated in the return section has been uniformly heated by compression.

In case A, the temperature at the level of the nozzle throat increases progressively as a result of a nonuniform heating of the air in the return section. At the time of starting, the mass of air near the injectors undergoes greater compression than the mass of air located in the collector, heating is greater there.

(b) Effect of Discharge

We compared two computation cases, case 1, where the exhaust flow was equal to the injected flow, and case 2, where the exhaust flow was lower than the injected flow.

The Mach number in the nozzle throat attains an asymptotic value in case 1, whereas in case 2 it goes through a maximum since the mass in the wind tunnel continues increasing.

The temperature in the nozzle throat rises substantially in case 2 due to the general compression of the circuit encountered at Piv.

(c) Effect of the Rise Time of Injection Pressure

The injection pattern was selected as follows:

$$P_{ij}/P_0 = 1 + 2.3\left(1 - e^{-\alpha \bar{t}}\right) \; ; \quad M_j = 0.7\left(P_{ij}/P_0 - 1\right)$$

We considered 2 values of α: 0.3 and 0.648. The injection temperature was the same as the flow temperature. The exhaust flow was selected so as to obtain the steady

state. The pressure-drop pattern was the same as in the case defined in paragraph IV.3.

We call attention to figure 16, where the greater α is the faster the increase of the Mach number.

We represented the temperature variations all along the system for $\bar{t} = 6$. It seems that by injecting at the same temperature as the flow we cannot expect to significantly reduce the temperature fluctuations by increasing the rise time of Pij. /17

For $\alpha = 0.3$, we obtain a rise time of q_j of the order of $\bar{t} = 5$, or 2/10 of a second for T'_2, which is already considerable bearing in mind the small gain in temperature fluctuations.

In conclusion, the preponderant effect of the rise time of Pij appears to be linked to the setting-up time of the Mach number in the throat. Compression and expansion causing fluctuations in the Mach number and in the temperature, which are not attenuated according to the computation, appear with higher values of α.

(d) Effect of Injection Temperature

We compared the case of injection at the same impact temperature as the flow with the case having an injection temperature peak quite close to that of the experiment conducted with the T'_2. The other parameters retain their values in both cases.

In figure 17 we see a definite improvement in temperature drop caused by the injection of hot air. This phenomenon can be understood by observing how the rates of

flow vary at the level of the injector, as well as temperature T_{i1} upstream of the injector in case 1.

It will be seen that flow q_j plays a leading role at the beginning of start-up, we virtually have $q_1 = 0$; $q_j = q_2$, since the drive ratio μ^{-1} tends little by little to its operating value. Temperature T_{i1} upstream of the injector starts dropping due to an expansion effect and then rises progressively. By suitably selecting the temperature peak, it is possible to maintain T_{i2} virtually constant, thus preventing the initial temperature drop upstream of the injector from spreading.

By these means we can expect to reduce the temperature fluctuation in the nozzle throat. One of the limits is derived from the pressure drop in the return section, which causes a variation of Tiv of the order of 5%, or about 1.5°C for the pressure drops caused. The damping of the system itself may reduce this value even more by a ratio of the order of 2, thus making it possible to expect a variation of Tiv of less than 1 degree.

APPENDIX

1. Transformation of the basic equations

If the following are used as variables:

$$\bar{\omega} = \frac{\omega}{\omega_0} \; ; \; \bar{\rho} = \frac{\rho}{\rho_0} \; ; \; U = \frac{u}{a_0} \; ; \; \bar{p} = \frac{p}{p_0} \; ; \; Z = \text{Log}\, \bar{p} \; ;$$

$$S = \frac{s}{c_p} \; ; \; \bar{t} = \frac{a_0 t}{L} \; ; \; \bar{x} = \frac{x}{L} \; ;$$

$$\bar{m}' = \frac{L\omega}{\rho_0 \omega_0 a_0} m' \; ; \quad \bar{f}' = \frac{L\omega}{\rho_0 \omega_0 a_0^2} f'$$

L = Length of the circuit

ω_o = Minimum cross section of the circuit

X_o = Variable X at moment t = 0

The equations become:

$$\frac{\partial(\bar{\rho}\bar{\omega})}{\partial \bar{t}} + \frac{\partial(\bar{\rho} U \bar{\omega})}{\partial \bar{x}} = \bar{m}'$$

$$\frac{\partial(\bar{\rho}\bar{\omega}U)}{\partial \bar{t}} + \frac{\partial\left(\bar{\rho}\bar{\omega}U^2 + \frac{\bar{p}}{\gamma}\bar{\omega}\right)}{\partial \bar{x}} = \frac{\bar{p}}{\gamma}\frac{d\bar{\omega}}{d\bar{x}} - \bar{f}' + \bar{m}'U$$

$$\frac{\partial(\bar{\rho}\bar{\omega}S)}{\partial \bar{t}} + \frac{\partial\left(\bar{\rho}\bar{\omega}US\right)}{\partial \bar{x}} = (\gamma - 1)\frac{\bar{p}U}{\bar{\rho}}\bar{f}' + S\bar{m}'$$

Or a system of the type

$$\frac{\partial \vec{f}}{\partial \bar{t}} + \frac{\partial \vec{F}}{\partial \bar{x}} = \vec{G}$$

2. Numerical method of solution

The MacCormack scheme is used

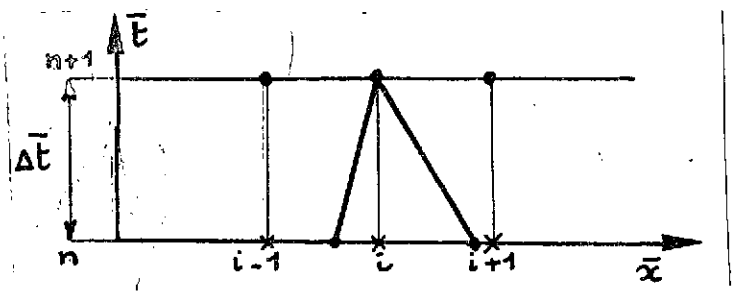

Let A_i^n be a magnitude at abscissa x_i and time t_n assumed to be known regardless of what i f_i^n, F_i^n, G_i^n is. /19

In order to determine f_i^{n+1}, we initially compute an approximate value of f_i^{n+1}, called $\tilde{f}$, according to the formula:

$$\tilde{f}_i^{n+1} = f_i^n - \frac{\Delta t}{\Delta x}\left(F_{i+1}^n - F_i^n\right) + \Delta t\, G_i^n$$

We then determine $\tilde{f}_i^{n+1}$ and $\tilde{G}_i^{n+1}$ from the preceding approximate values $\tilde{f}_i^{n+1}$.

For a value of f_i^{n+1} we then have

$$f_i^{n+1} = \frac{1}{2}\left\{f_i^n + \tilde{f}_i^{n+1} - \frac{\Delta t}{\Delta x}\left(\tilde{F}_{i-1}^{n+1} - \tilde{F}_i^{n+1}\right) + \Delta t\, \tilde{G}_i^{n+1}\right\}$$

as a second order approximation of f_i^{n+1}

In order to have the computation converge, it is necessary to ensure that the low values of the characteristics passing at moment t_{n+1} past point x_i are on the segment x_{i+1} X_{i-1} with relation to time t_n.

3. Treatment of injector discontinuity

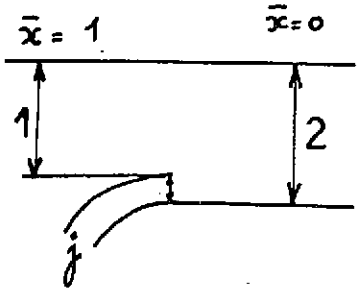

$$\begin{cases} \rho_1 u_1 \omega_1 + \rho_j u_j \omega_j = \rho_2 u_2 \omega_2 \\ \left(p_1 + \rho_1 u_1^2\right)\omega_1 + \left(p_j + \rho_j u_j^2\right)\omega_j = \left(p_2 + \rho_2 u_2^2\right)\omega_2 \\ h_{i1}\, q_1 + h_{ij}\, q_j = h_{i2}\, q_2 \end{cases}$$

In order to determine the conditions at (2) knowing the conditions at (1), we have to solve

$$\begin{cases} \rho_2 u_2 = A \\ p_2 + \rho_2 u_2^2 = B \\ h_{i2} = C \end{cases} \quad \text{with } h_{i2} = \frac{a_2^2}{\gamma - 1} + \frac{u_2^2}{2}$$

Eliminating ρ and a we have:

$$\frac{\gamma+1}{2(\gamma-1)}u^2 - \frac{\gamma}{\gamma-1}\frac{B}{A}u + C = 0$$

Assuming

$$\bar{A} = A/\rho_0 a_0 \; ; \; \bar{B} = B/\rho_0 a_0^2 \; ; \; \bar{h}_i = h_i/a_0^2$$

u is then the solution of a quadratic equation; therefore the solution corresponding to the absence of shock is for γ = 1.4. /20

$$u = \left(3{,}5\,\bar{B}/\bar{A} - \sqrt{3{,}5^2(\bar{B}/\bar{A})^2 - 12\,\bar{h}_i}\right)\frac{1}{6}$$

If $\bar{A}$ is small, it is better to calculate first $\bar{\rho} = \frac{\bar{A}}{u}$

by $$\bar{\rho} = \frac{1}{2\bar{h}_i}\left(3{,}5\,\bar{B} + \sqrt{3{,}5^2\bar{B}^2 - 12\,\bar{h}_i\bar{A}^2}\right)$$

then $$u = \frac{\bar{A}}{\bar{\rho}} \quad et \quad \bar{p} = \gamma\left(\bar{B} - \bar{A}u\right)$$

4. Loss patterns

1. In the steady state, losses $\frac{dp_i}{\rho_i}$ must be linked to the df appearing in equations

$$(1)\quad d(\rho\omega u) = dm$$

$$(2)\quad d\left(\omega(p+\rho u^2)\right) = p\,d\omega - df + u\,dm$$

$$(3)\quad d\,h_i = 0 = T\,ds + \frac{dp}{\rho} + u\,du$$

Taking into account equation (1), equation (2) yields

$$\omega\left(dp + \rho u\,du\right) = -df$$

or

$$df = -\omega\rho\,\frac{dp_i}{p_i}$$

$f' = \frac{df}{dx}$ is therefore known if we know ρ_i (x).

2. In the unsteady case, we assumed $\frac{dp_i}{\rho_i}$ to be proportional to u^2.

REFERENCES

/21

[1] Carriere, P., Lecture Series on Large Transonic Wind Tunnels, Institut. Von Karman, January 1973.

[2] Schnitt, V., Experimental Study of Internal Noise in Induction Wind Tunnels [Estude experimental du brüit interne dans les souffleries a induction], La Recherche Aerospatiale, No. 1973-6, Nov. - Dec.

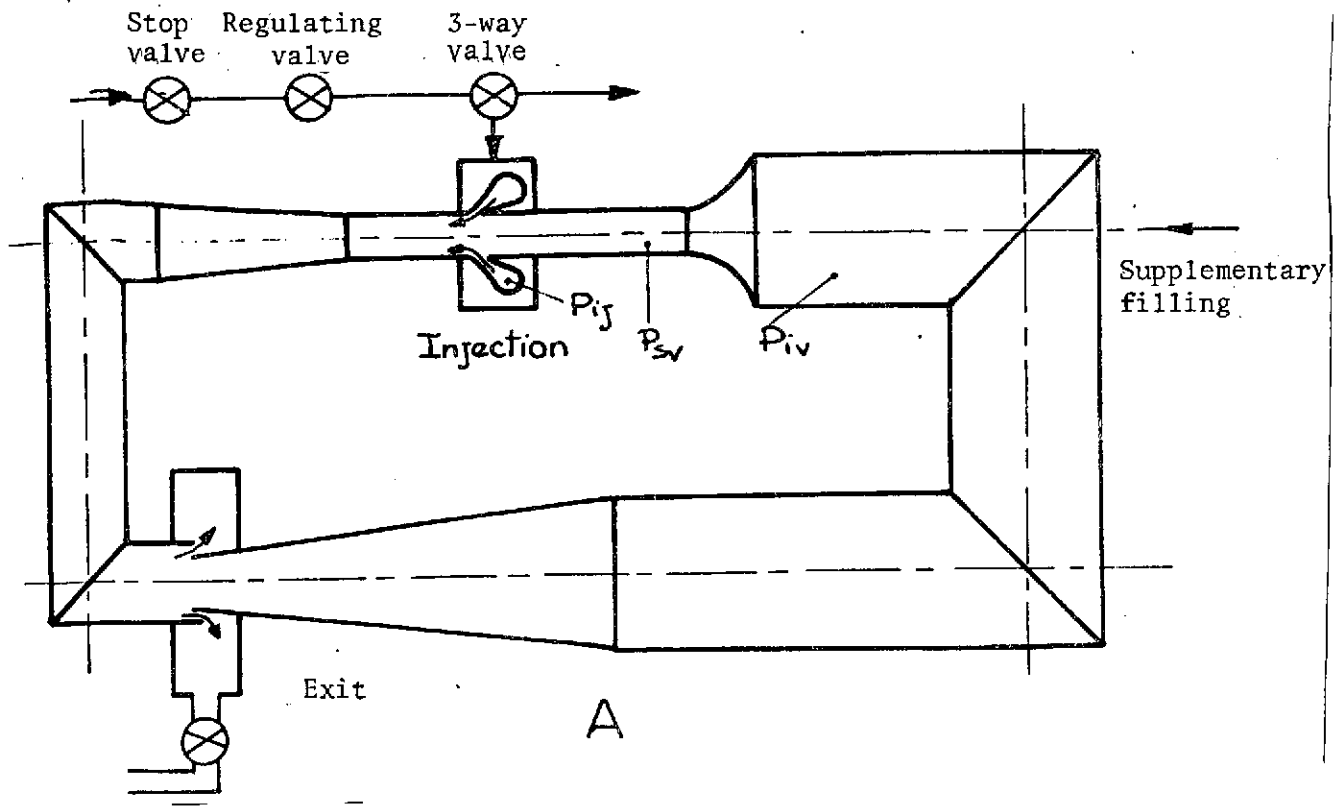

A

B et C

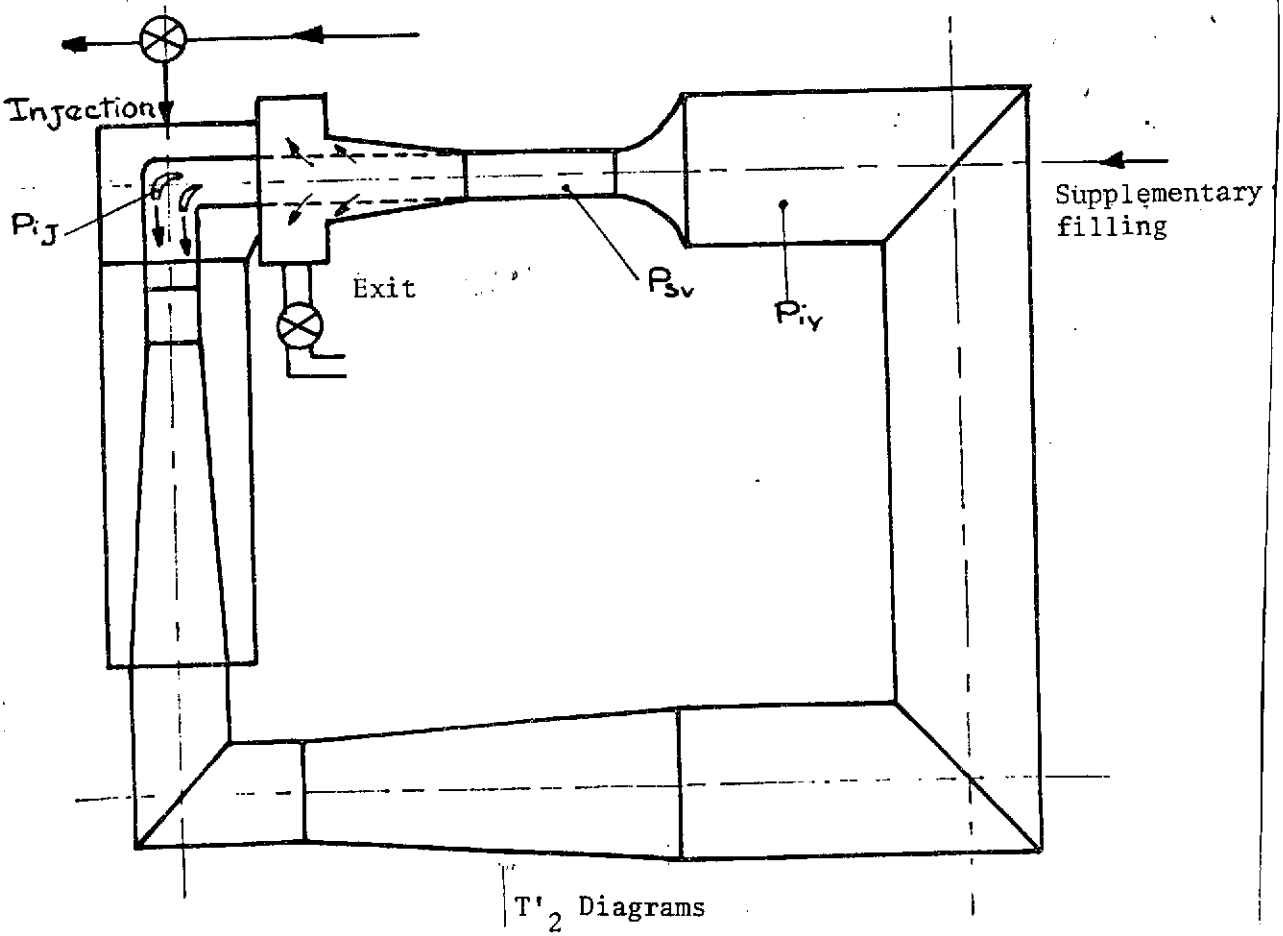

T'_2 Diagrams

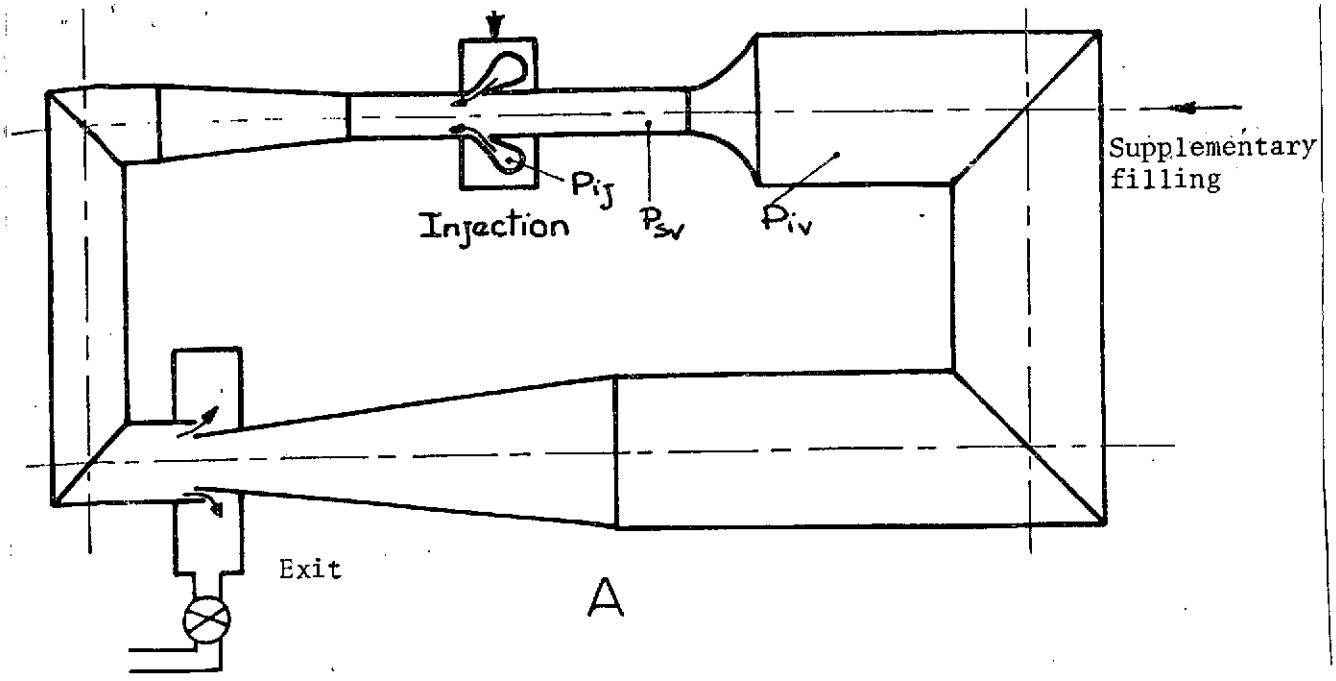
Supplementary filling
Injection
P_{ij}
P_{sv}
P_{iv}
Exit
A

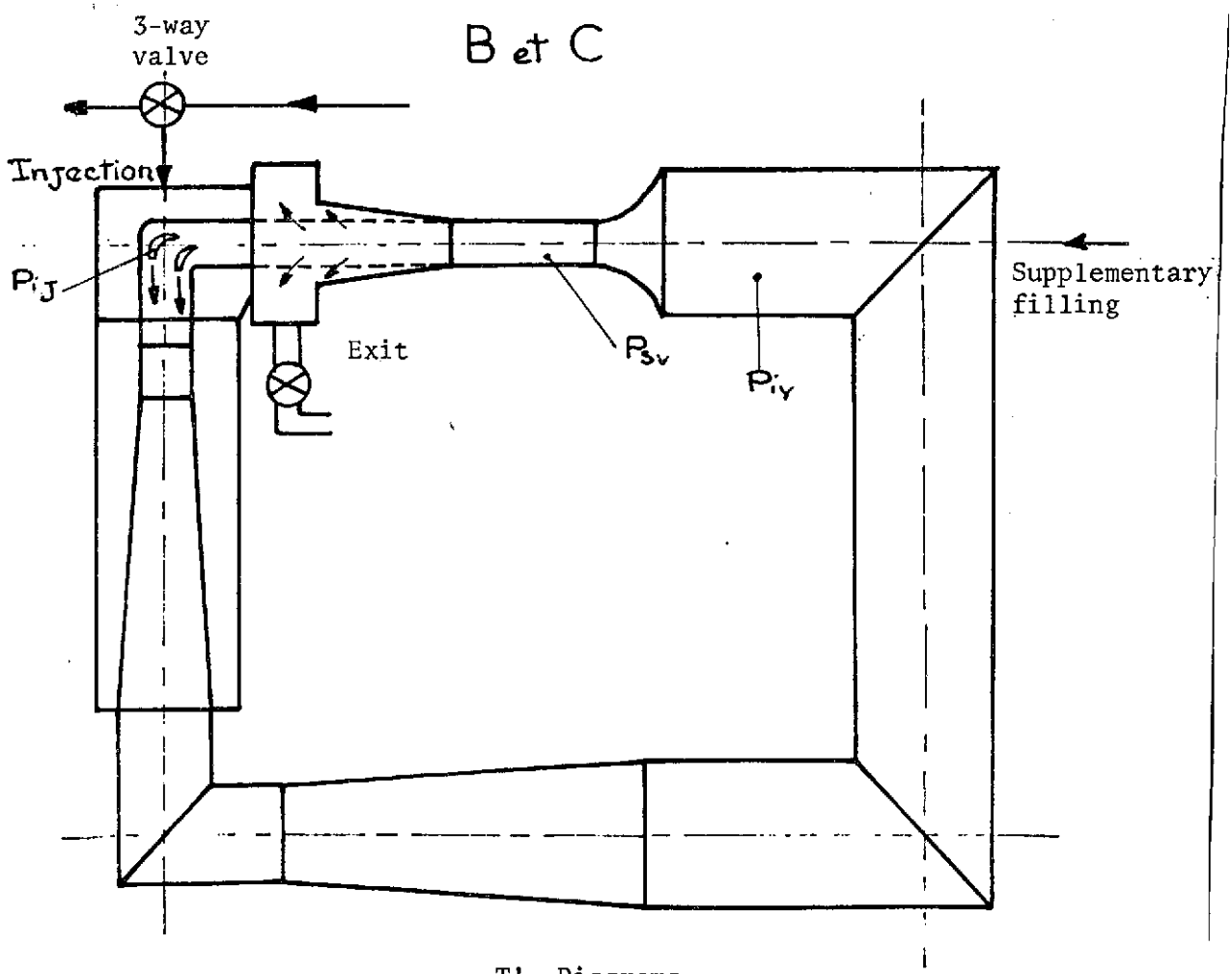
B et C
3-way valve
Injection
P_{ij}
Exit
P_{sv}
P_{iv}
Supplementary filling

T'_2 Diagrams

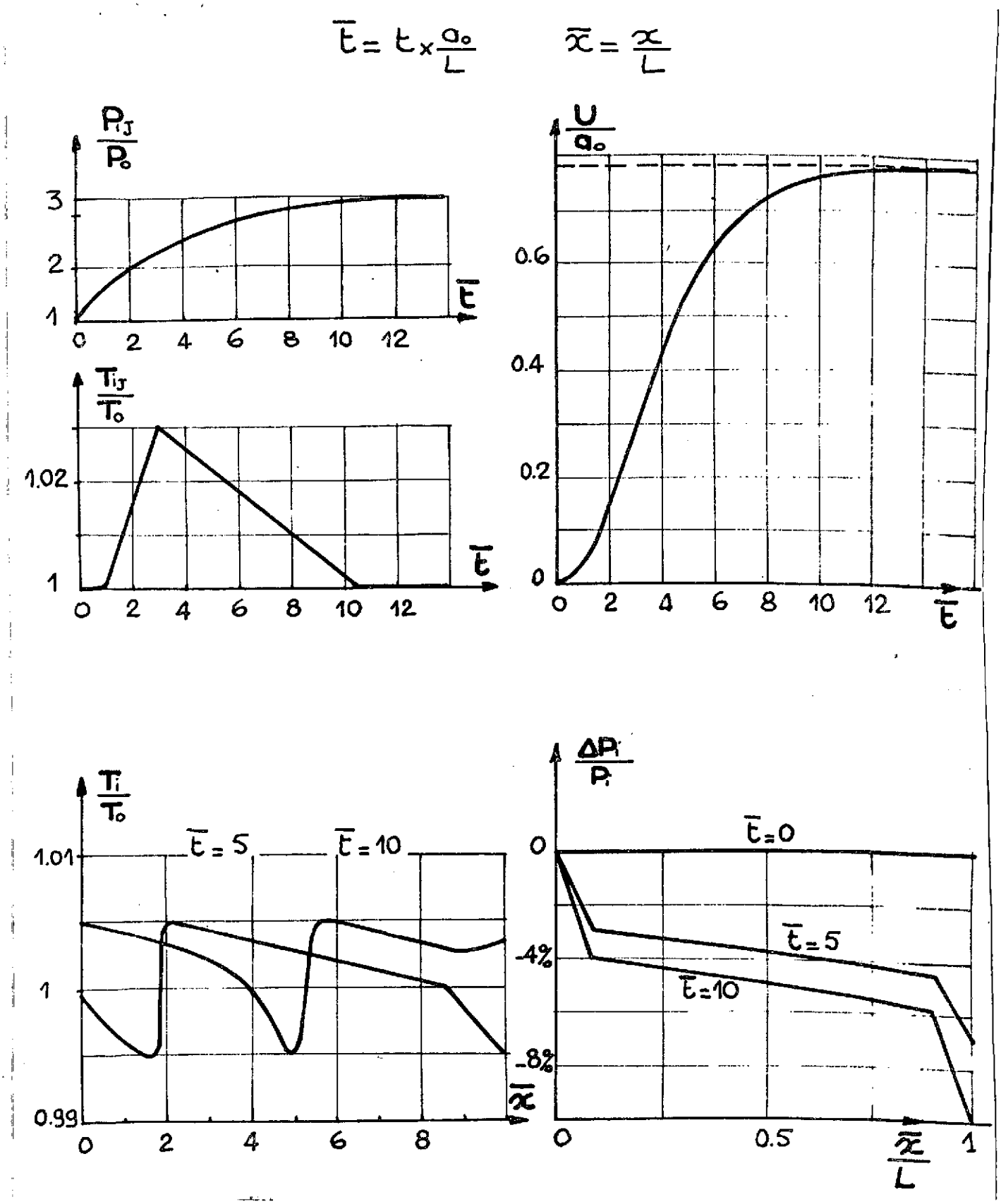

BASIC PHENOMENA OBTAINED BY NUMERICAL COMPUTATION

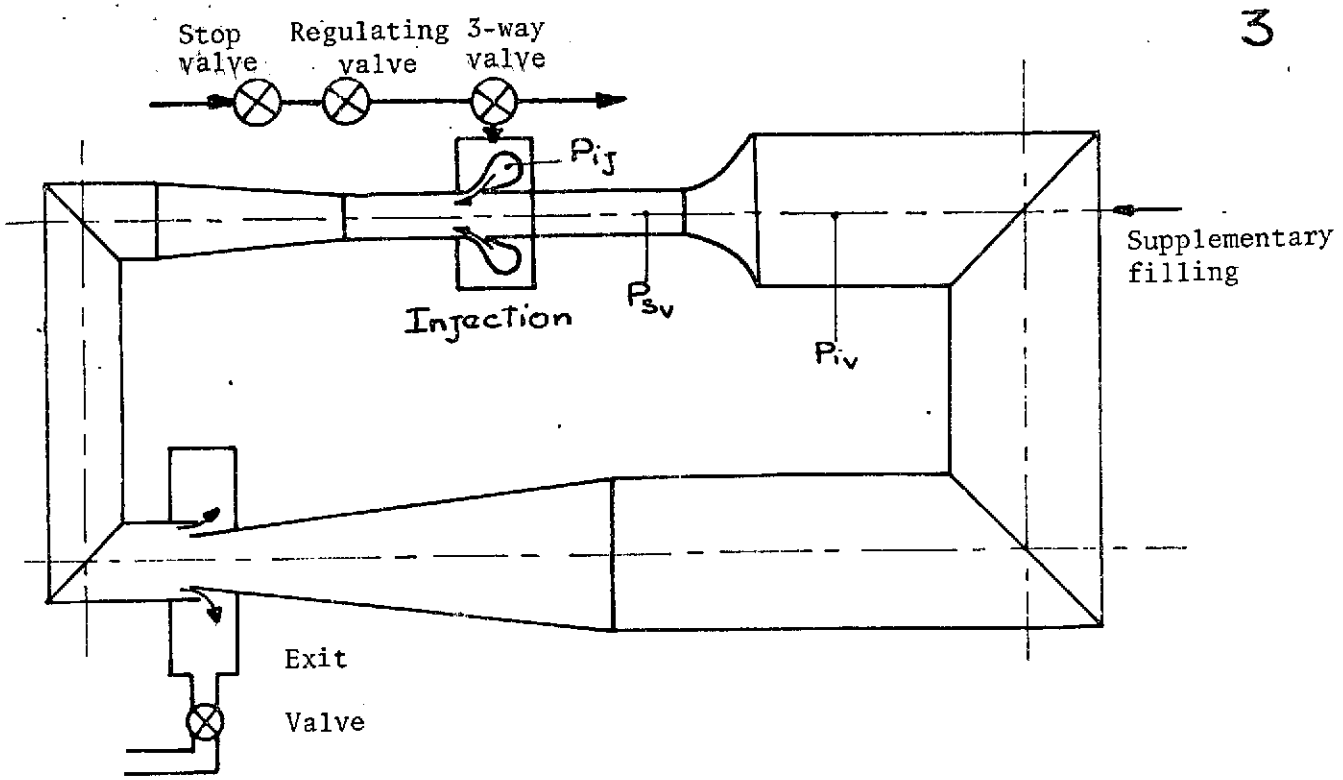
Stop valve
Regulating valve
3-way valve
P_{ij}
Injection
P_{sv}
P_{iv}
Supplementary filling
Exit
Valve

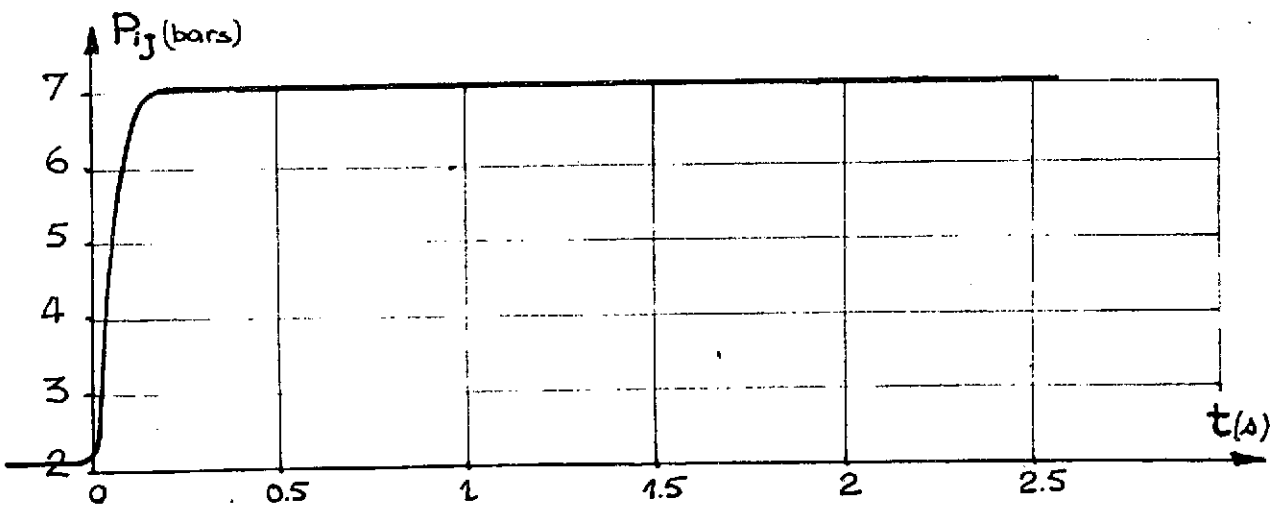
P_{ij} (bars)
7
6
5
4
3
2
0
0.5
1
1.5
2
2.5
t(s)

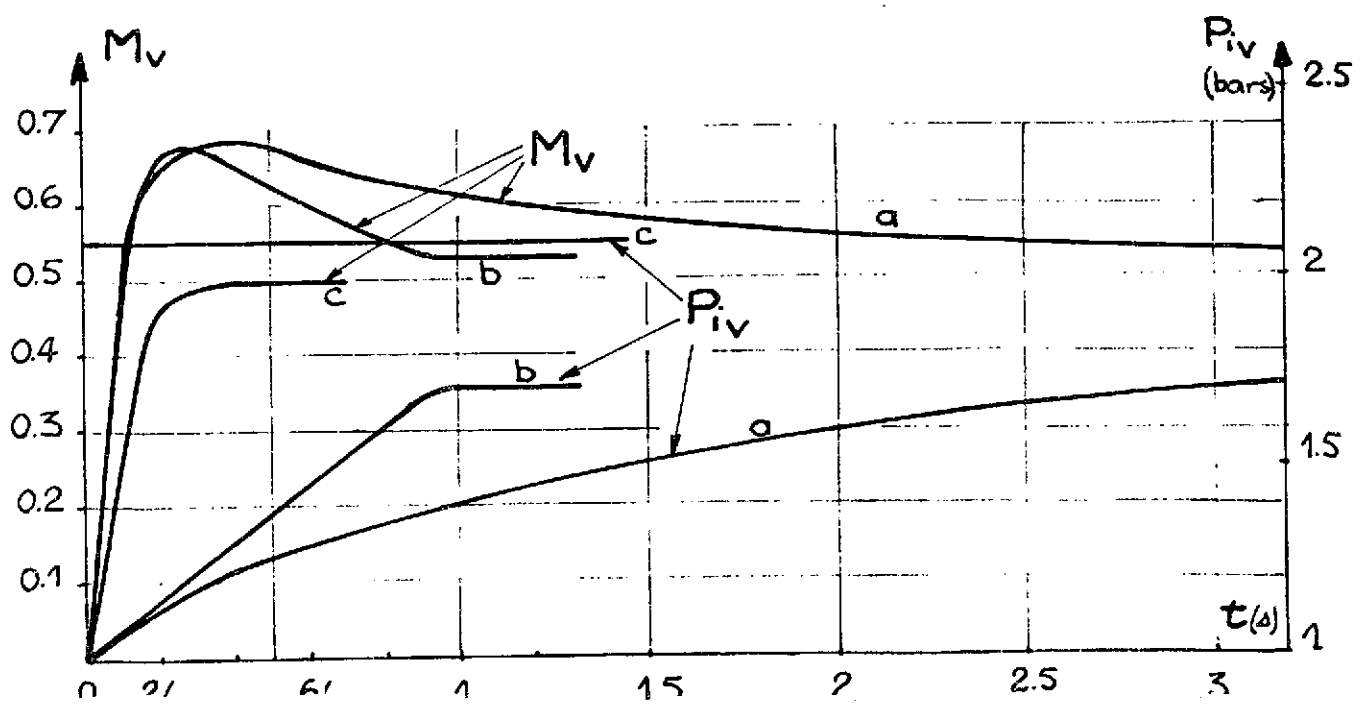
M_v
0.7
0.6
0.5
0.4
0.3
0.2
0.1
M_v
a
b
c
c
b
P_{iv}
a
P_{iv} (bars)
2.5
2
1.5
1
t(s)
0
0.5
1
1.5
2
2.5
3

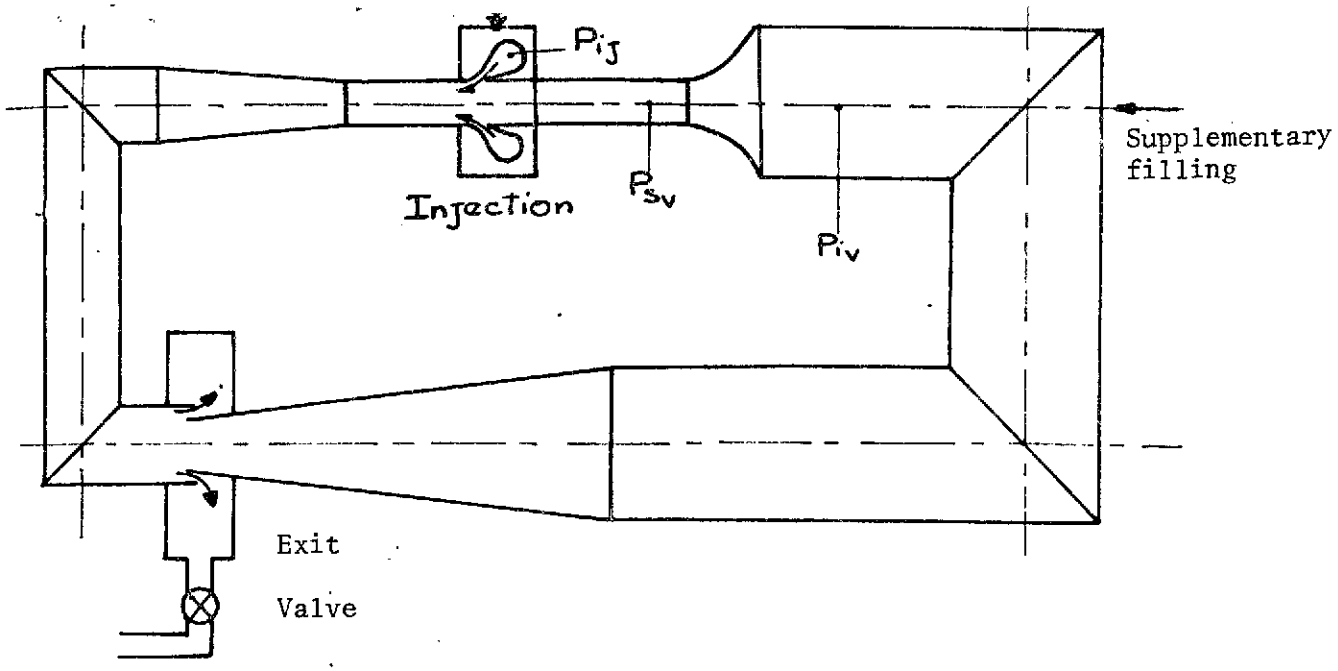
P_{ij}
Injection
P_{sv}
P_{iv}
Supplementary filling
Exit
Valve

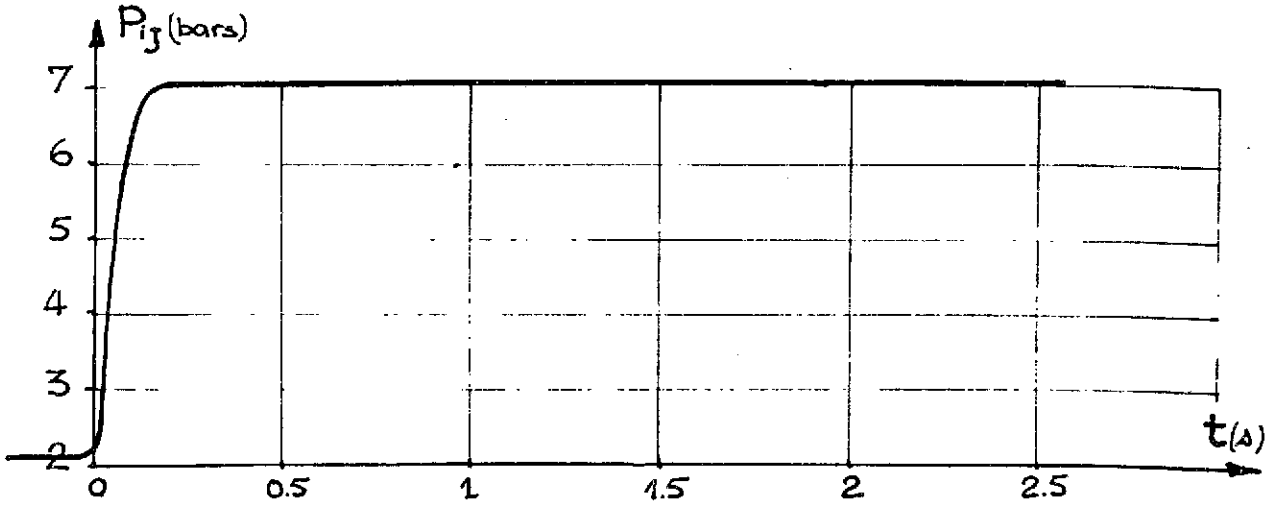
P_{ij} (bars)
7
6
5
4
3
2
0
0.5
1
1.5
2
2.5
t(s)

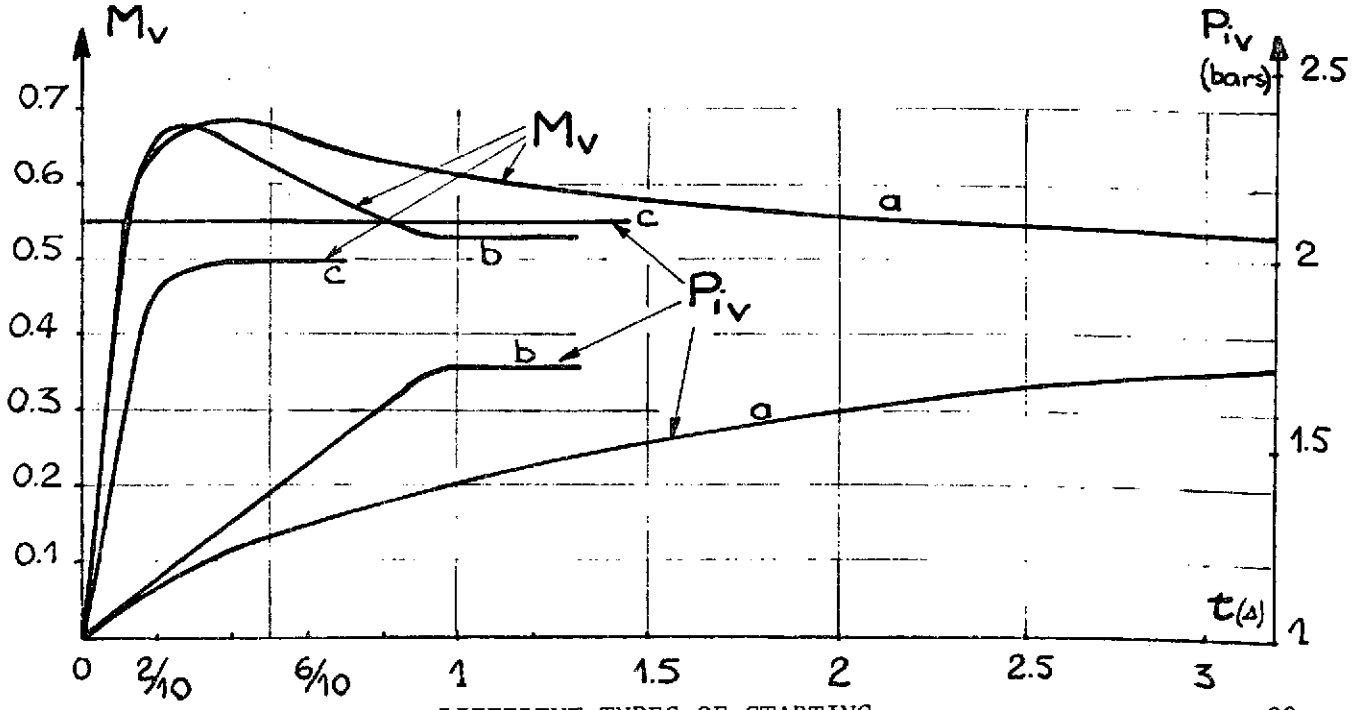
M_v
P_{iv} (bars)
0.7
0.6
0.5
0.4
0.3
0.2
0.1
2.5
2
1.5
1
M_v
a
b
c
c
b
P_{iv}
a
t(s)
0
2/10
6/10
1
1.5
2
2.5
3

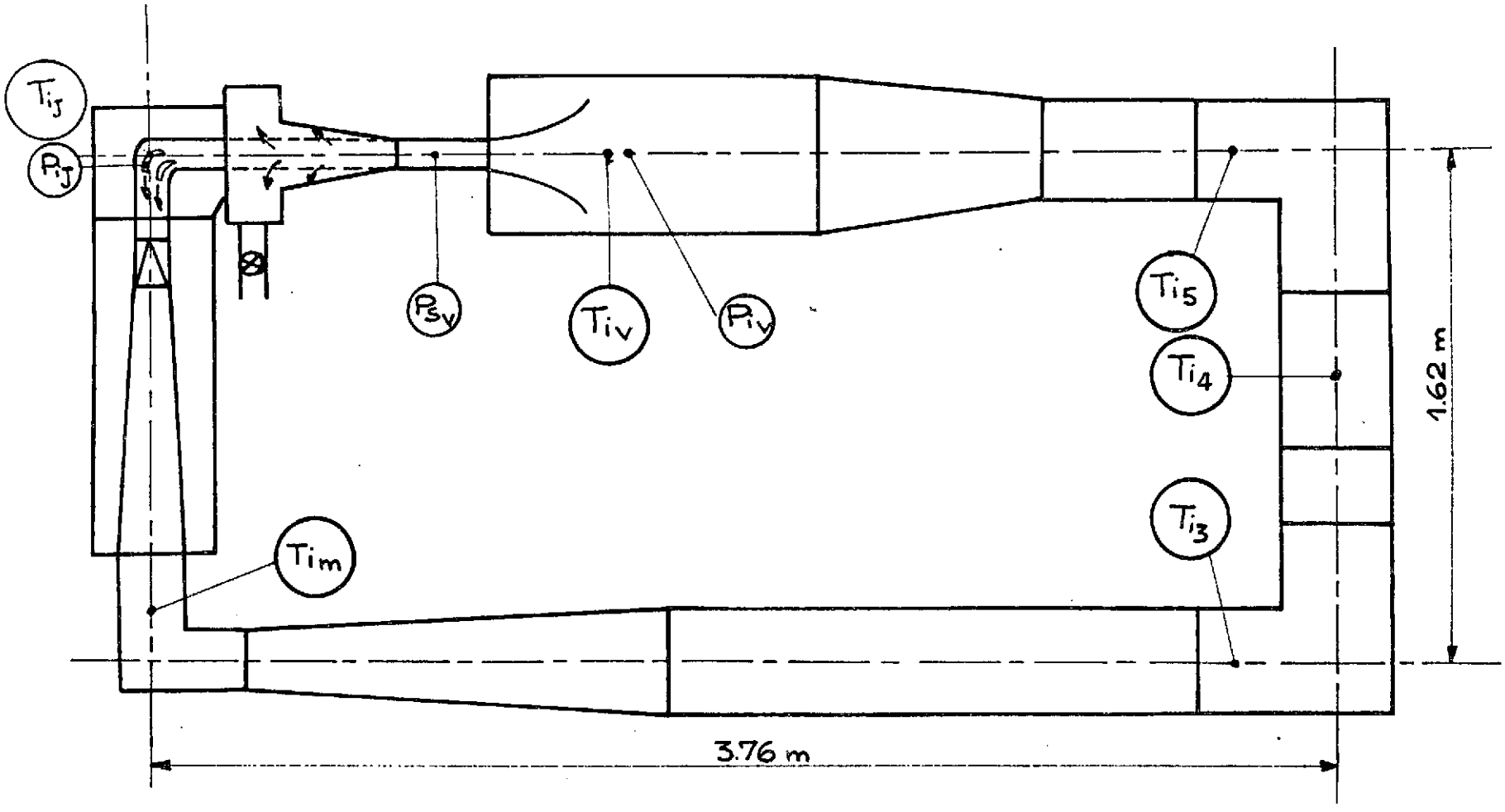

POSITIONS OF PRESSURE AND TEMPERATURE PROBES

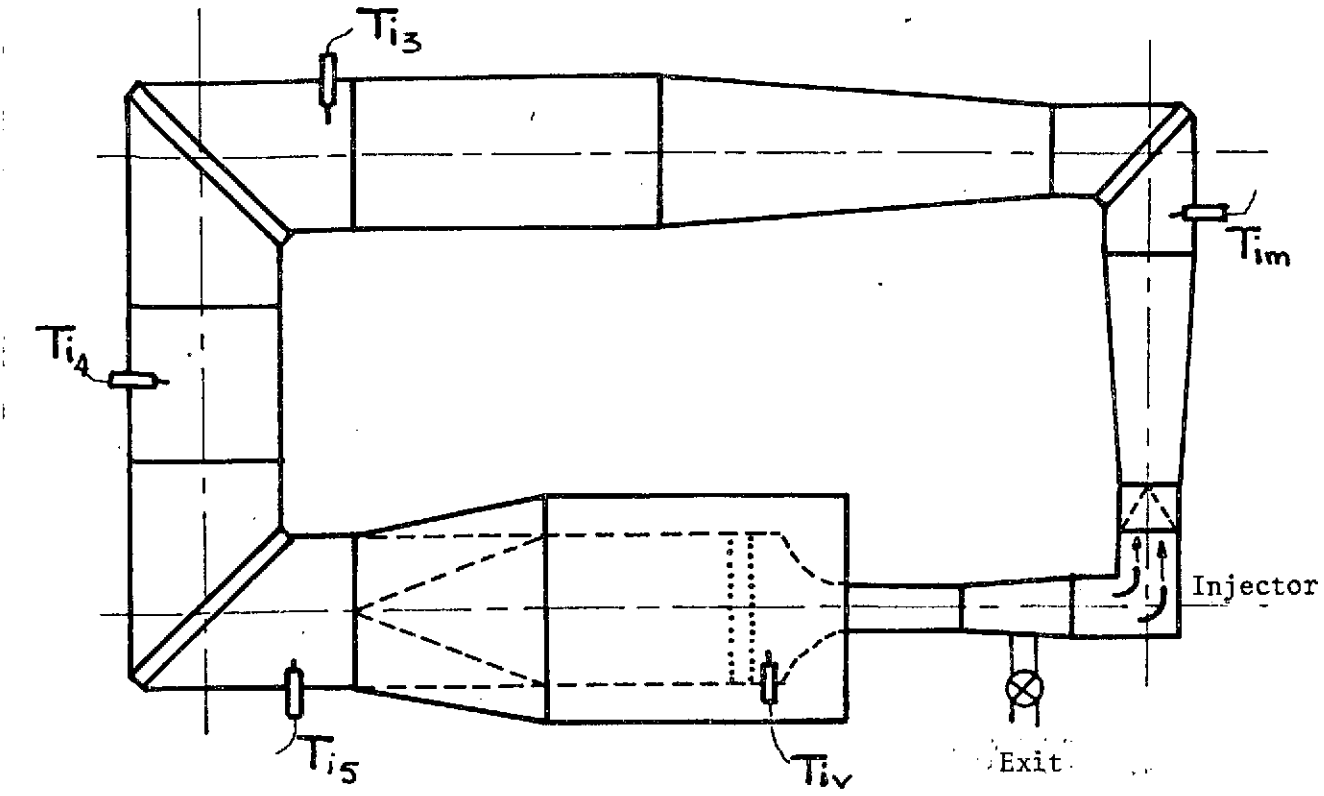

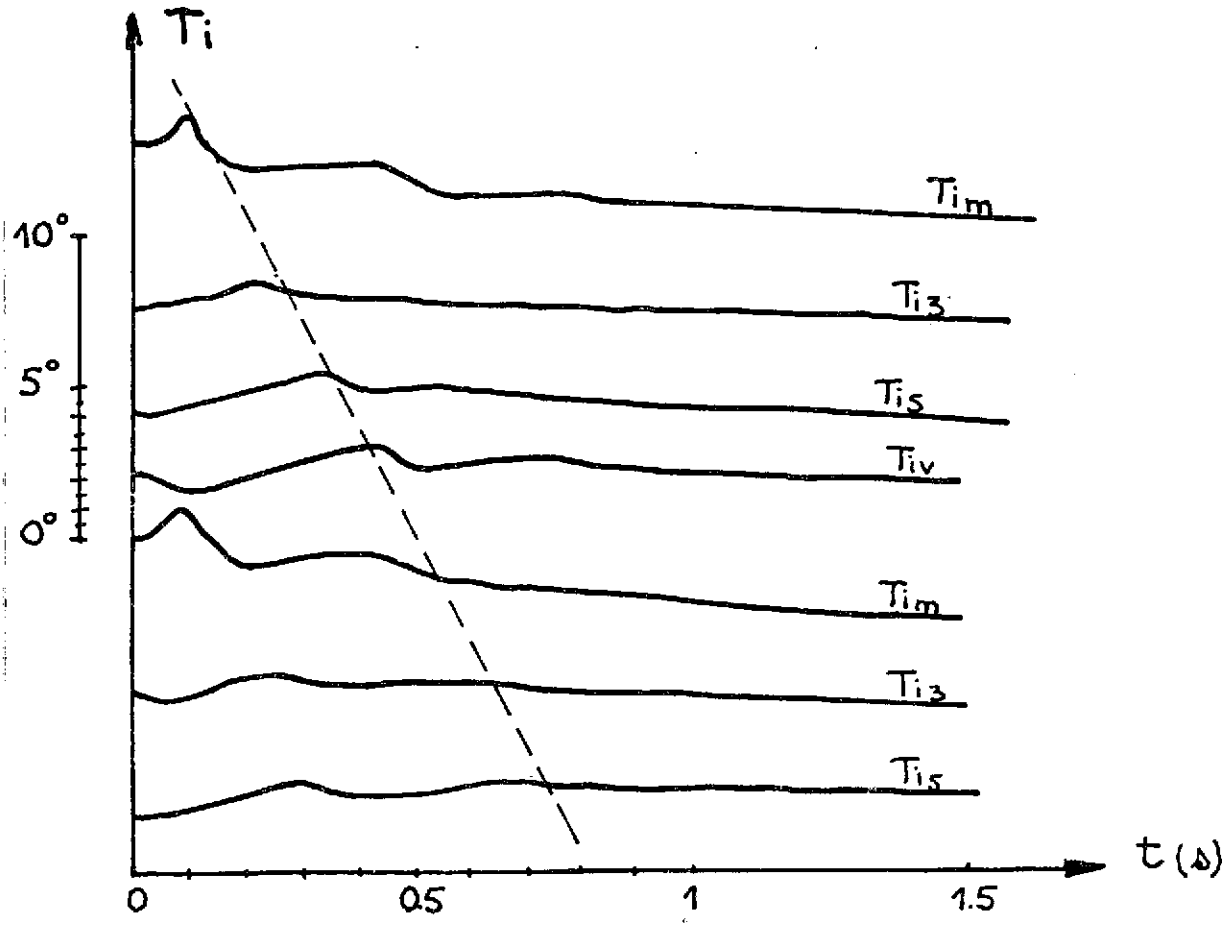

TEMPERATURE DEVELOPMENT

EFFECT OF A PRESSURE DROP

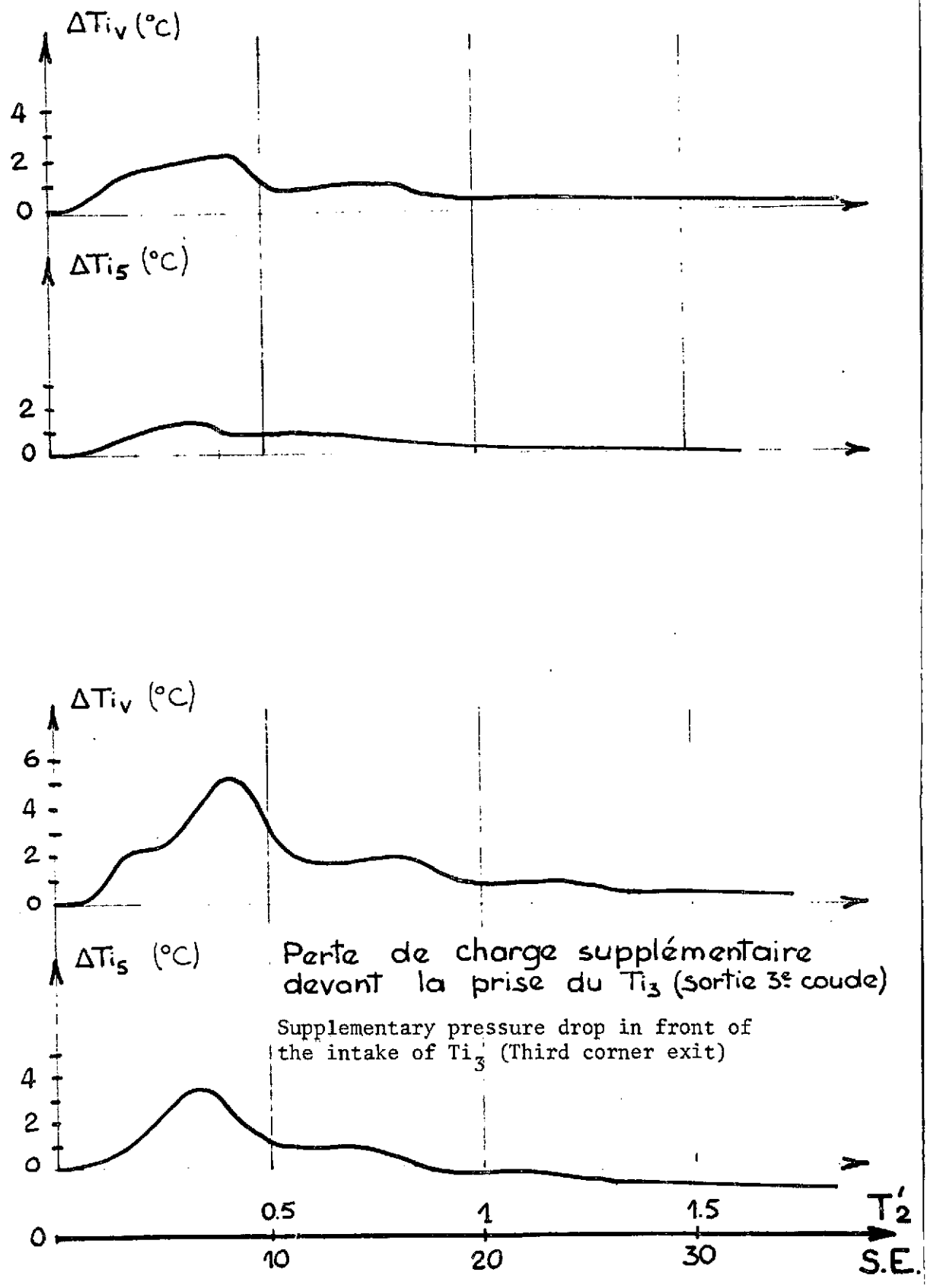

EFFECT OF THE SHIFT OF INLET-OUTLET OPENINGS

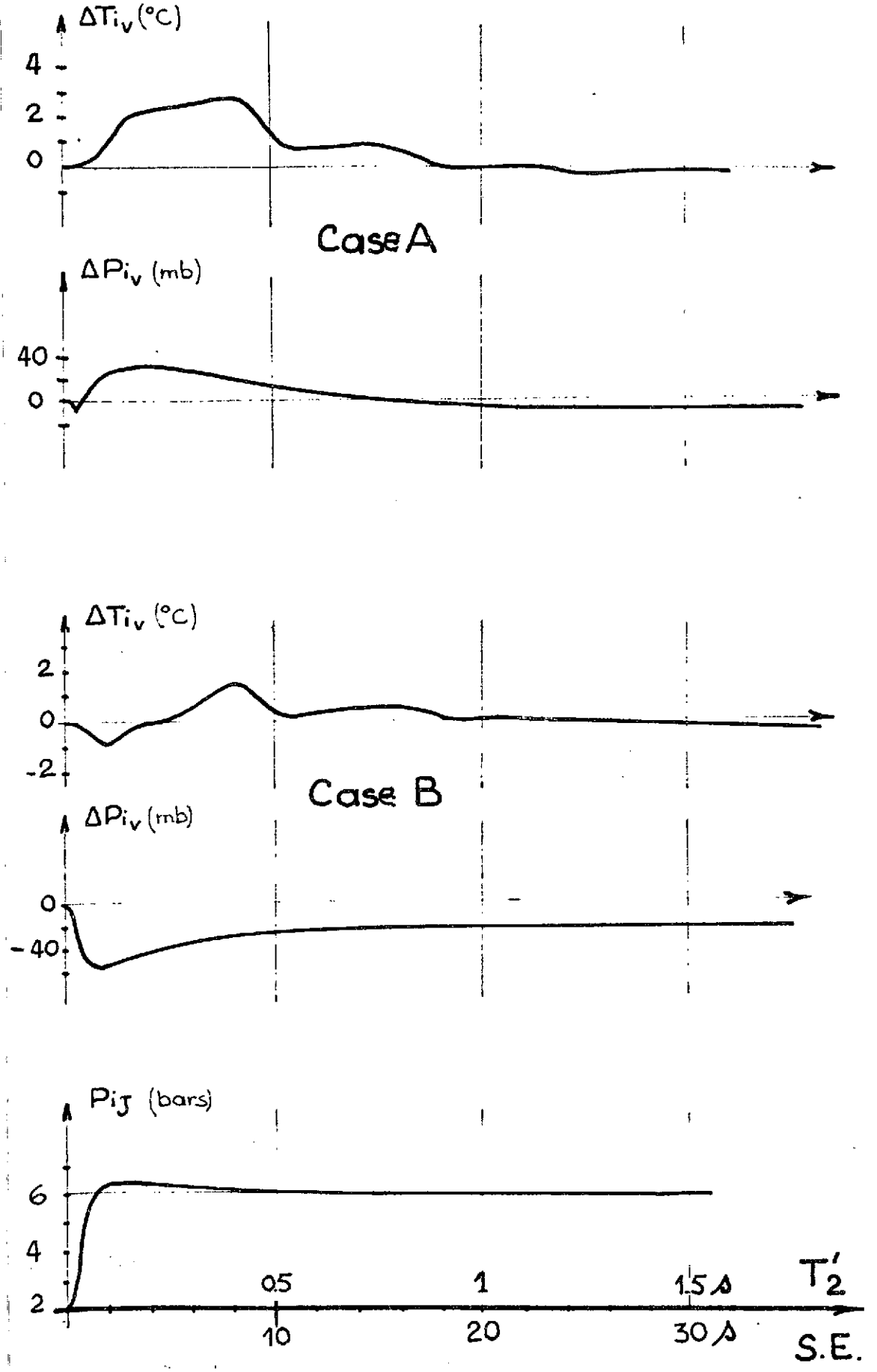

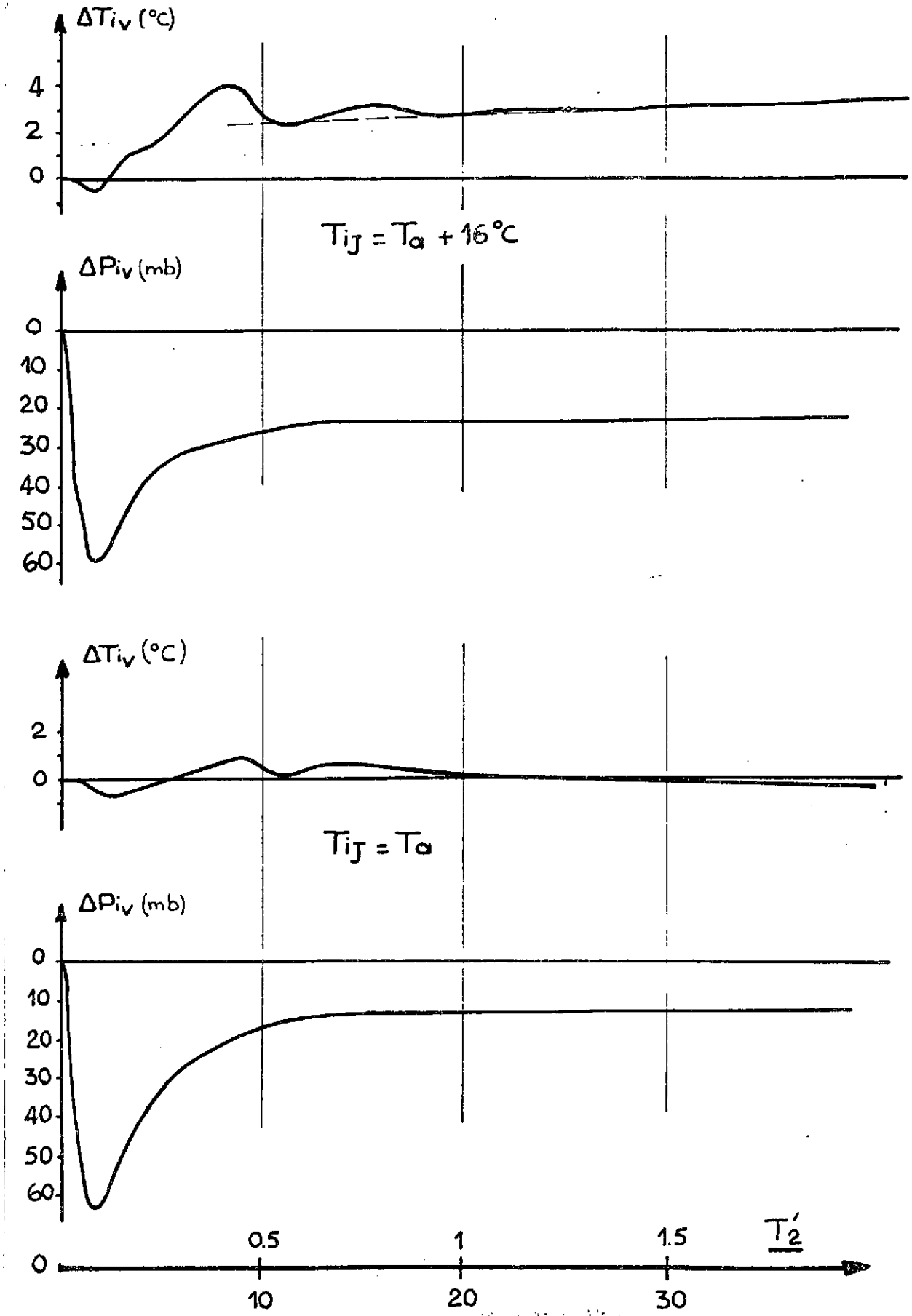
ΔTiv (°C)
4
2
0
Tij = Ta + 16°C
ΔPiv (mb)
0
10
20
30
40
50
60
ΔTiv (°C)
2
0
Tij = Ta
ΔPiv (mb)
0
10
20
30
40
50
60
0.5
1
1.5
T'2
0
10
20
30

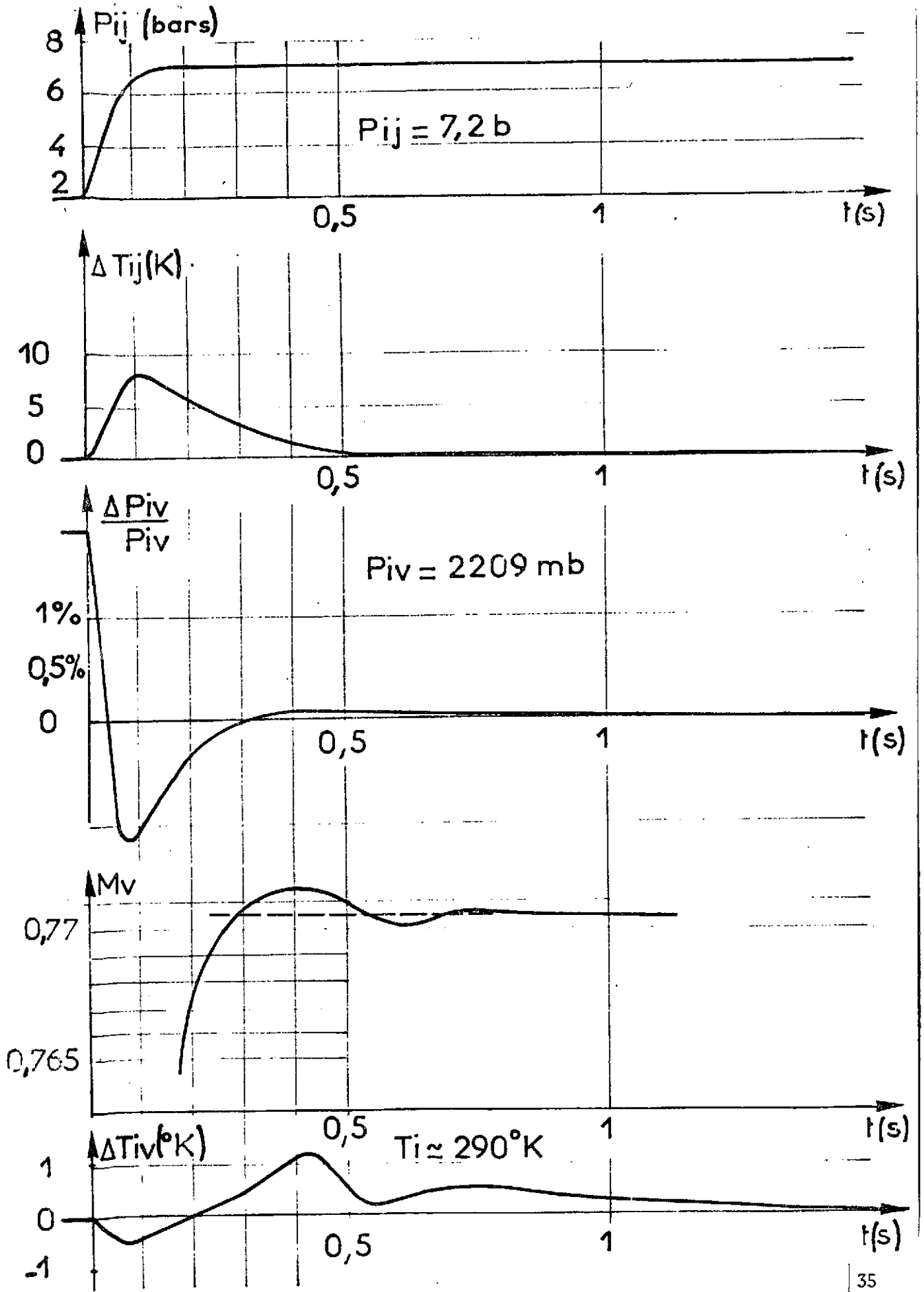

PRESENTATION OF A TYPICAL TEST WITH THROAT

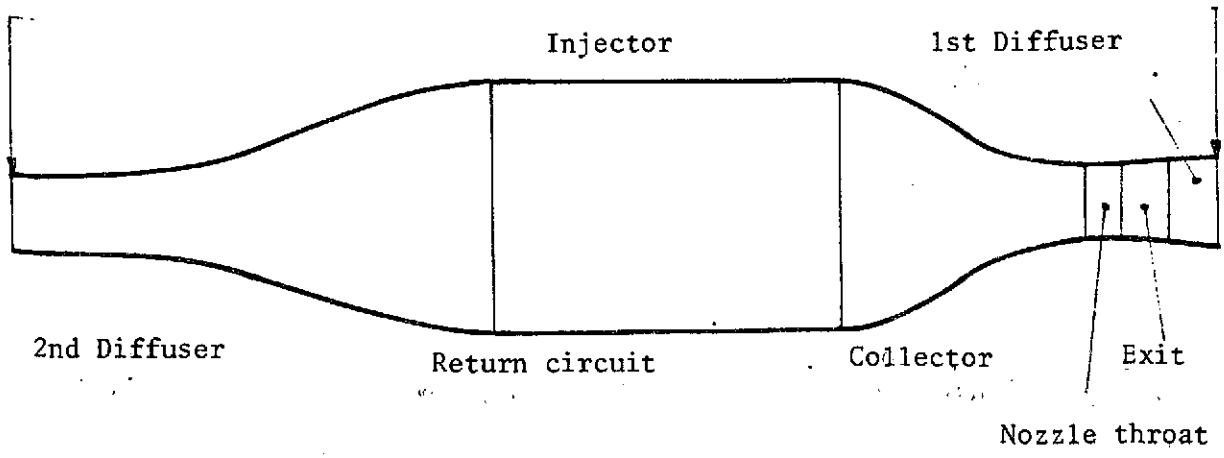

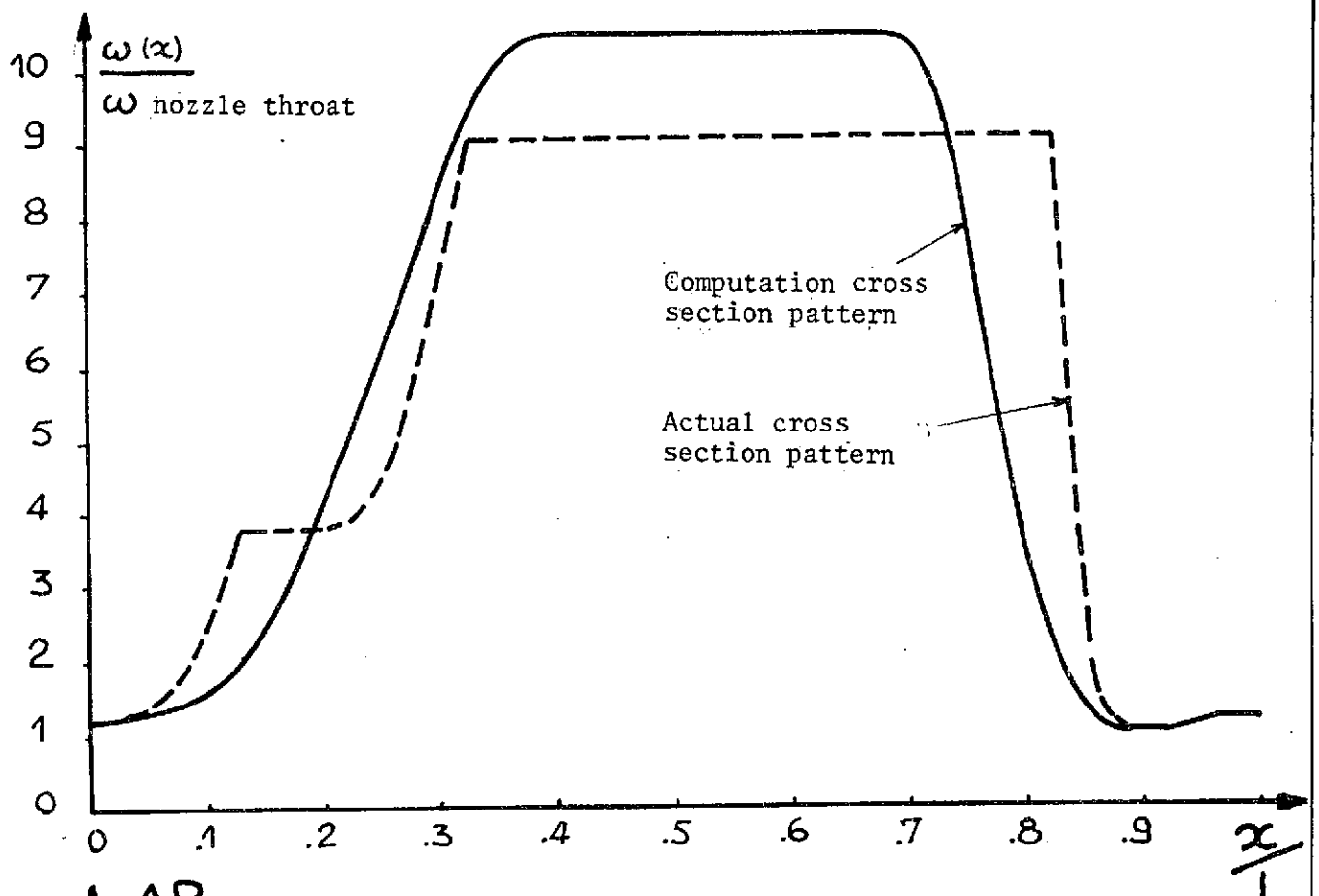

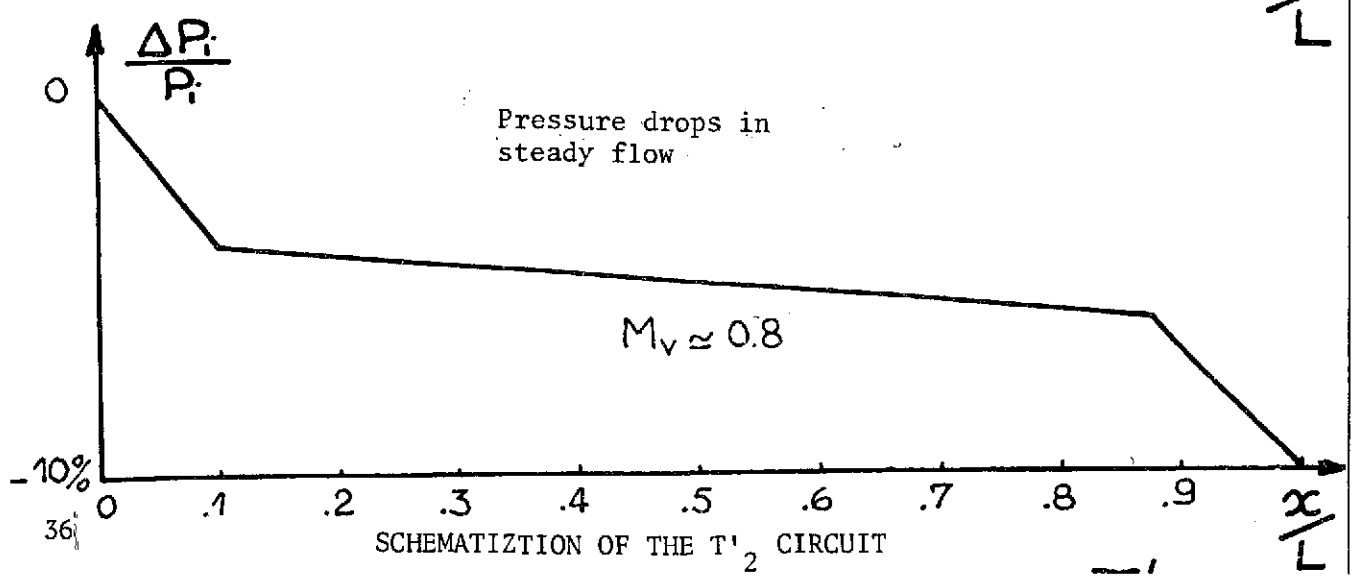

SCHEMATIZTION OF THE T'$_2$ CIRCUIT

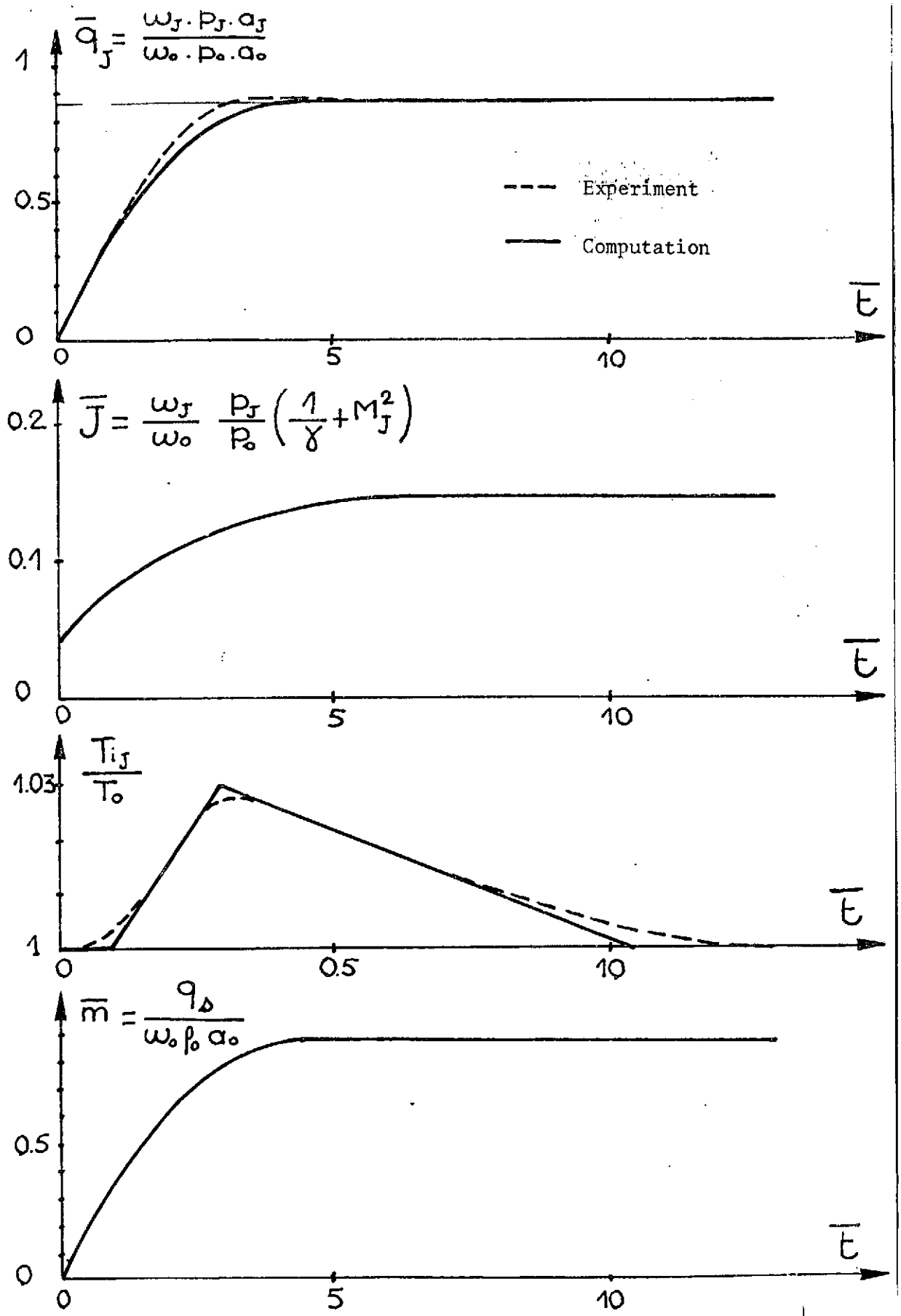
$\bar{q}_J = \frac{\omega_J \cdot p_J \cdot a_J}{\omega_0 \cdot p_0 \cdot a_0}$
1
0.5
0
0
5
10
Experiment
Computation
$\bar{t}$
$\bar{J} = \frac{\omega_J}{\omega_0} \frac{p_J}{p_0} \left(\frac{1}{\gamma} + M_J^2 \right)$
0.2
0.1
0
0
5
10
$\bar{t}$
$\frac{T_{iJ}}{T_0}$
1.03
1
0
0.5
10
$\bar{t}$
$\bar{m} = \frac{q_\Delta}{\omega_0 \rho_0 a_0}$
0.5
0
0
5
10
$\bar{t}$

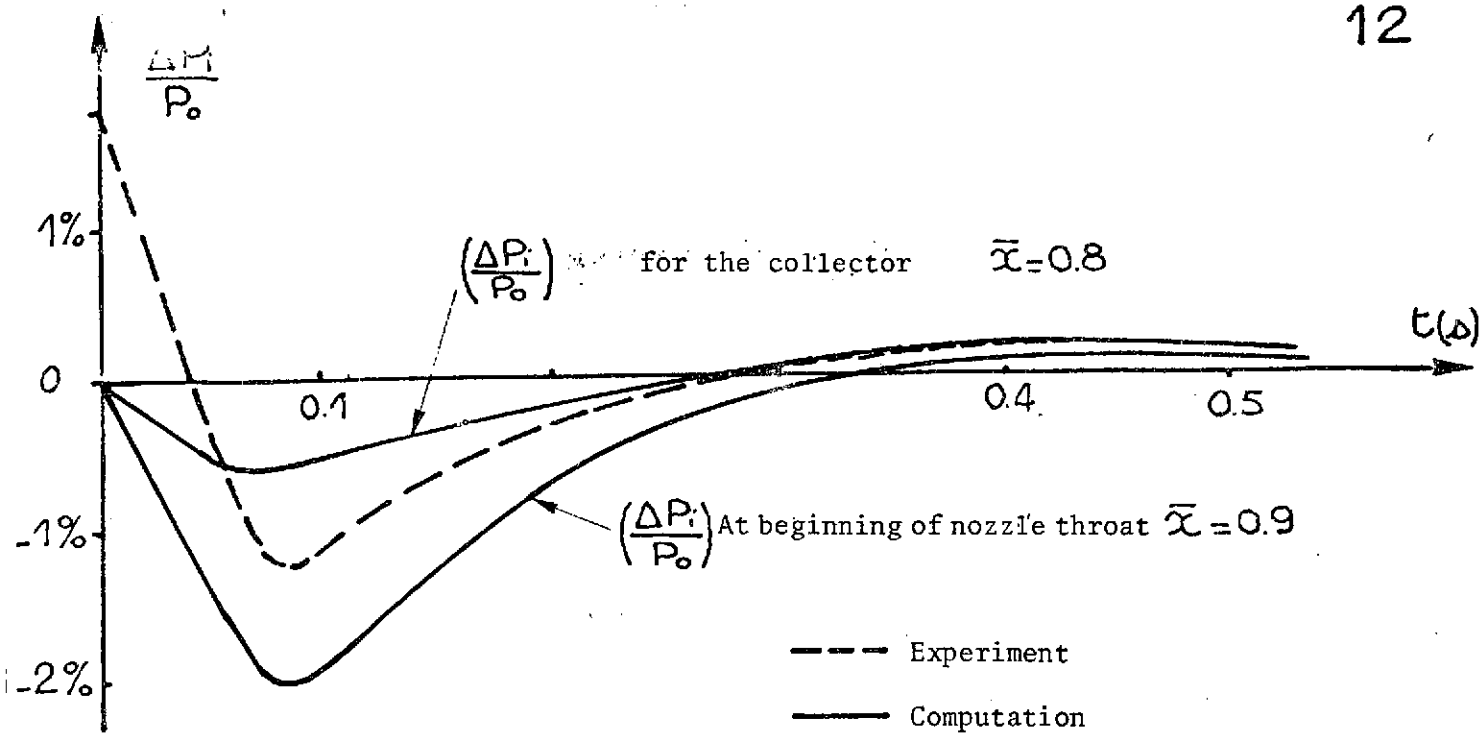

Variation of nozzle-throat pressure

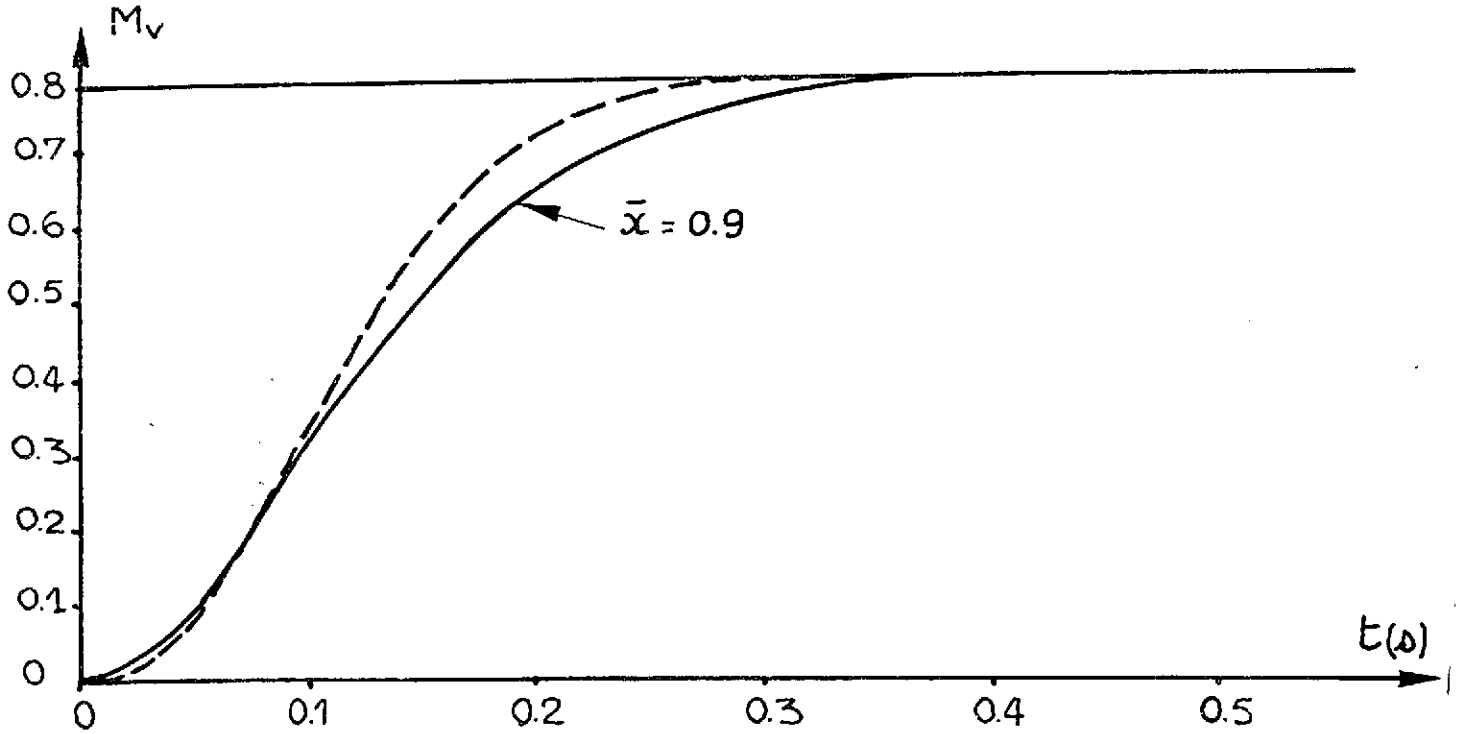

Nozzle-throat Mach number as a function of time

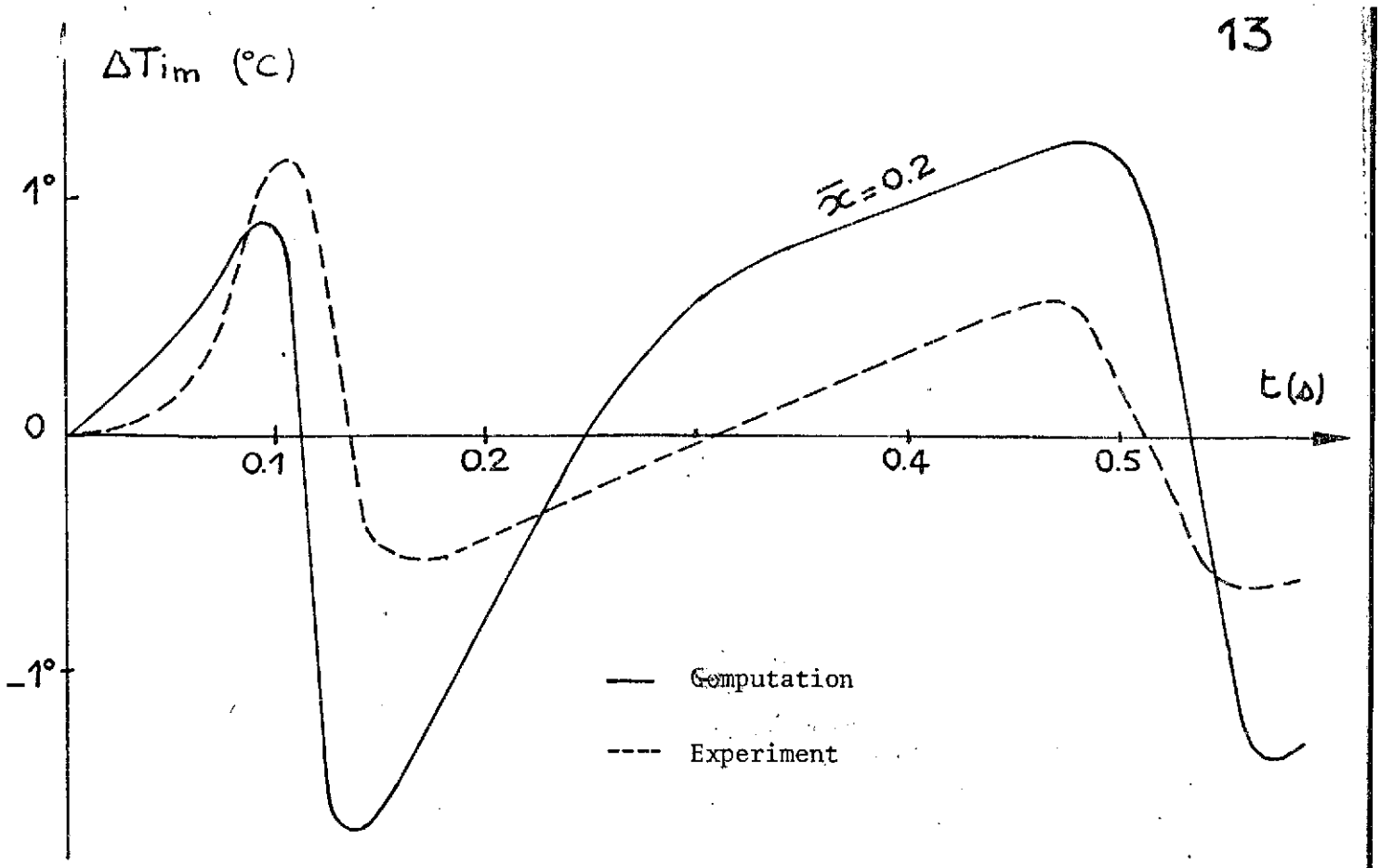
ΔTim (°C)
1°
0
-1°
0.1
0.2
0.4
0.5
t(s)
x̄=0.2
Computation
Experiment

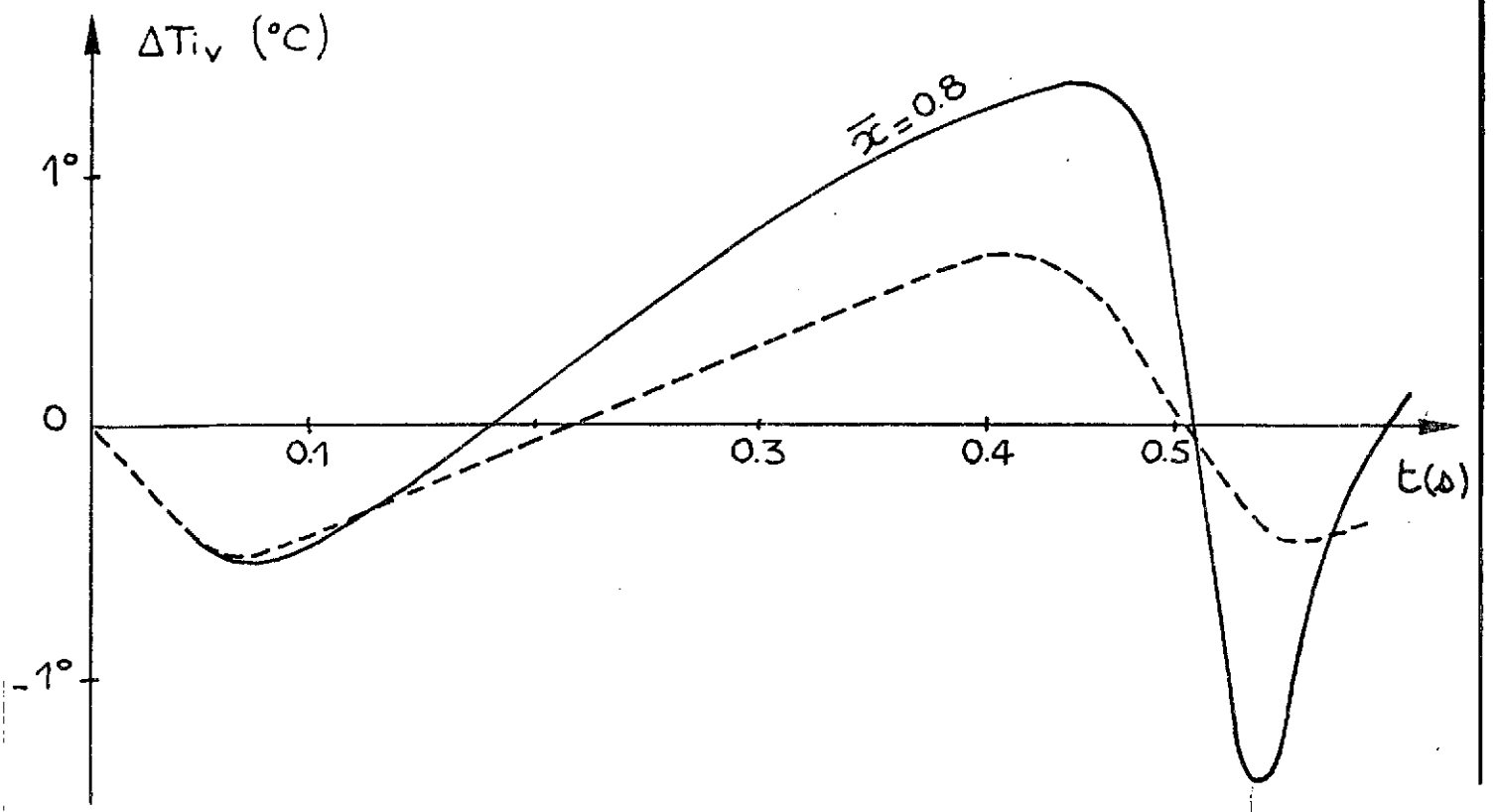
ΔTiv (°C)
1°
0
-1°
0.1
0.3
0.4
0.5
t(s)
x̄=0.8

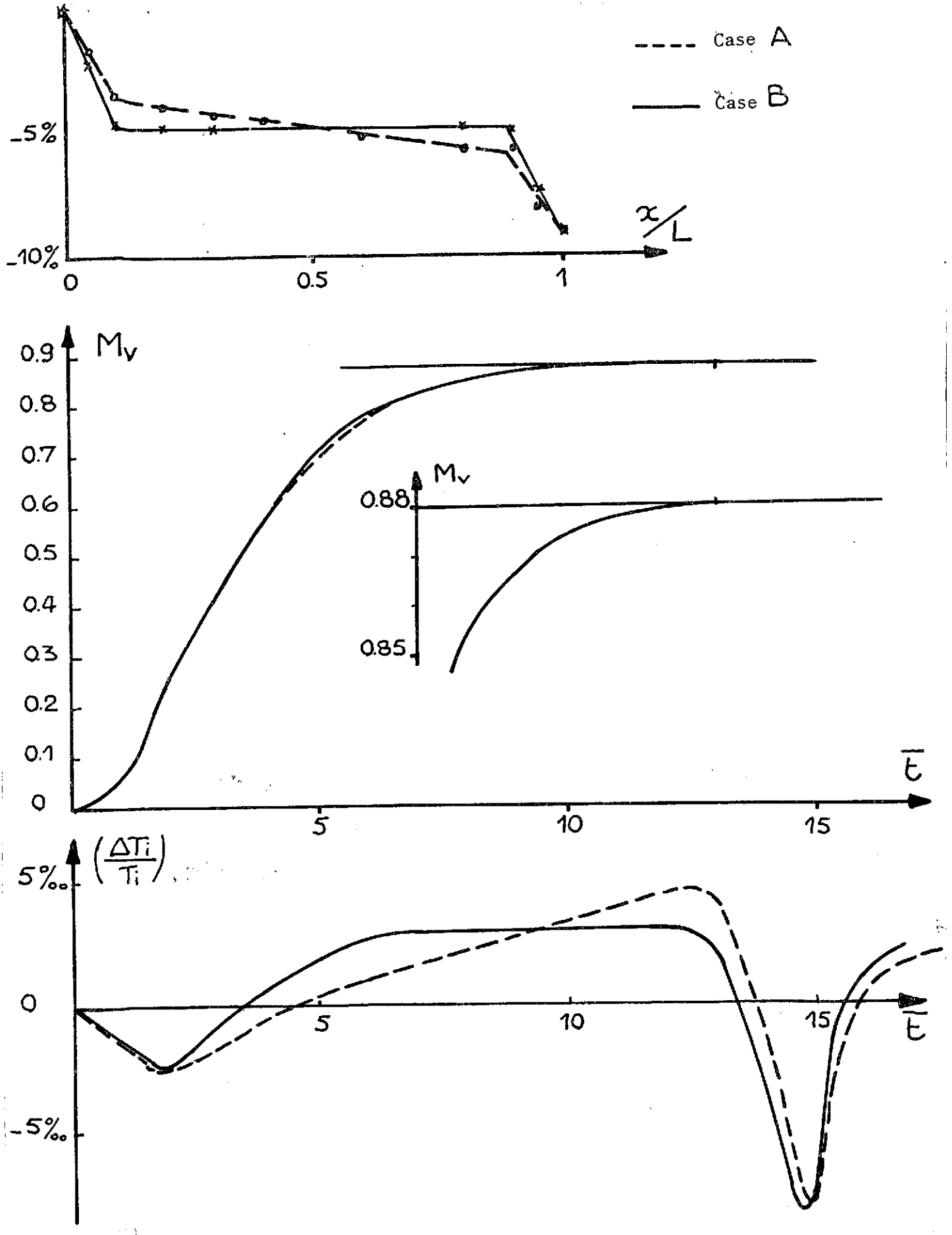
Case A
Case B
-5%
-10%
0
0.5
1
x/L
0.9
0.8
0.7
0.6
0.5
0.4
0.3
0.2
0.1
0
Mv
0.88
0.85
5
10
15
t
5‰
0
-5‰
(ΔTi/Ti)

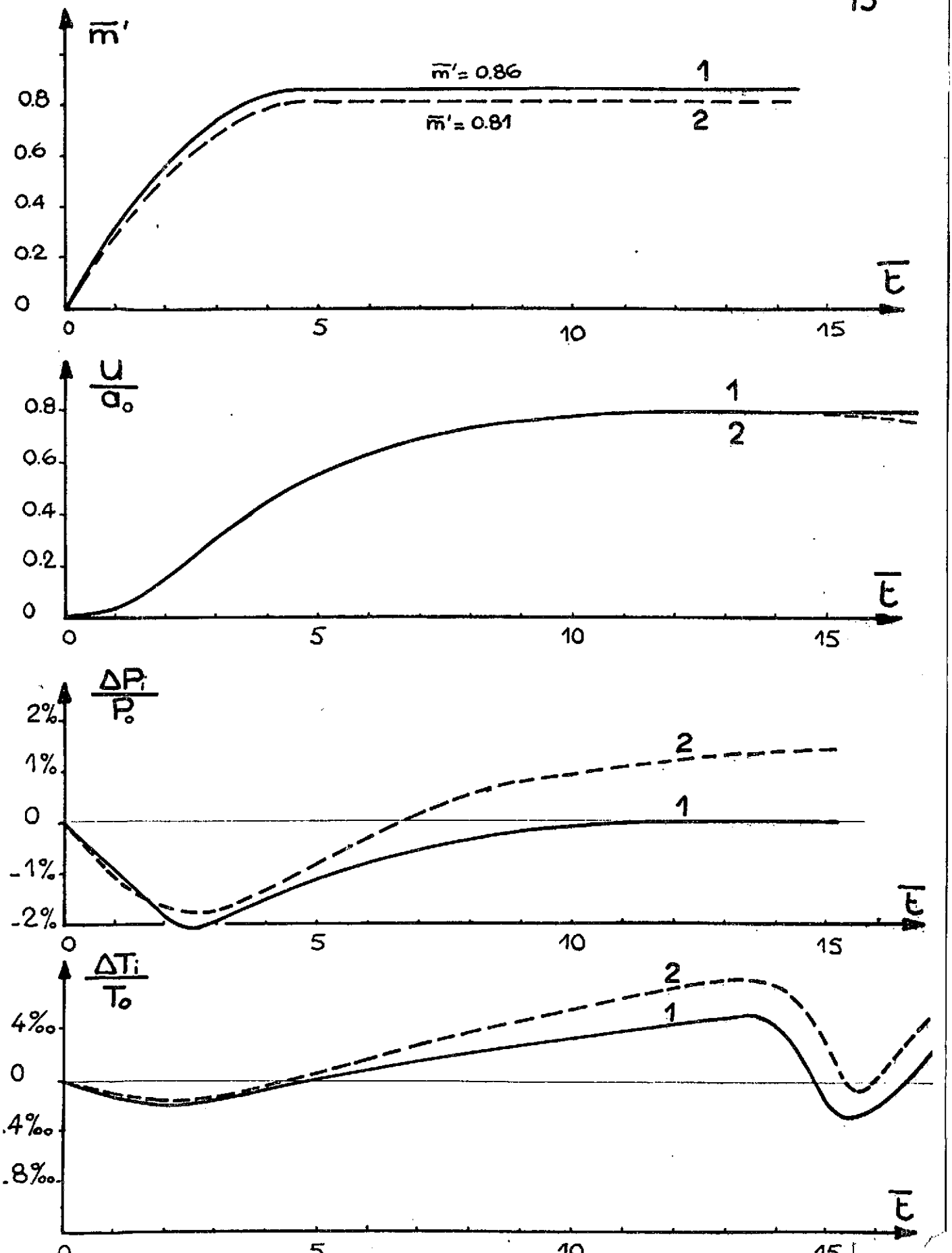
$\bar{m}'$
$\bar{m}' = 0.86$
1
$\bar{m}' = 0.81$
2
0.8
0.6
0.4
0.2
0
$\bar{t}$
0
5
10
15
$\frac{U}{a_0}$
0.8
0.6
0.4
0.2
0
1
2
$\bar{t}$
0
5
10
15
$\frac{\Delta P_i}{P_0}$
2%
1%
0
-1%
-2%
2
1
$\bar{t}$
0
5
10
15
$\frac{\Delta T_i}{T_0}$
4‰
0
.4‰
.8‰
2
1
$\bar{t}$
0
5
10
15

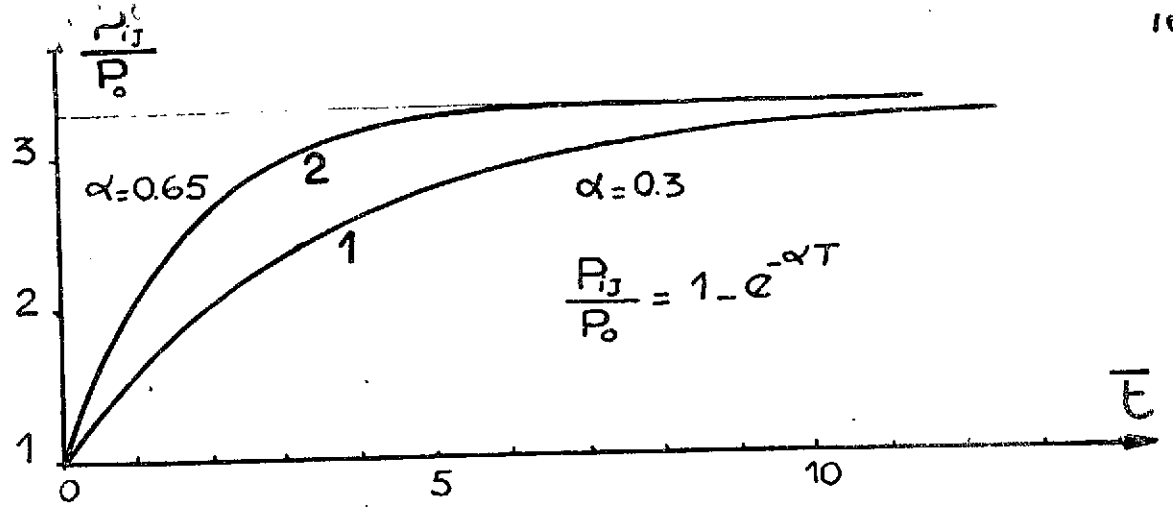

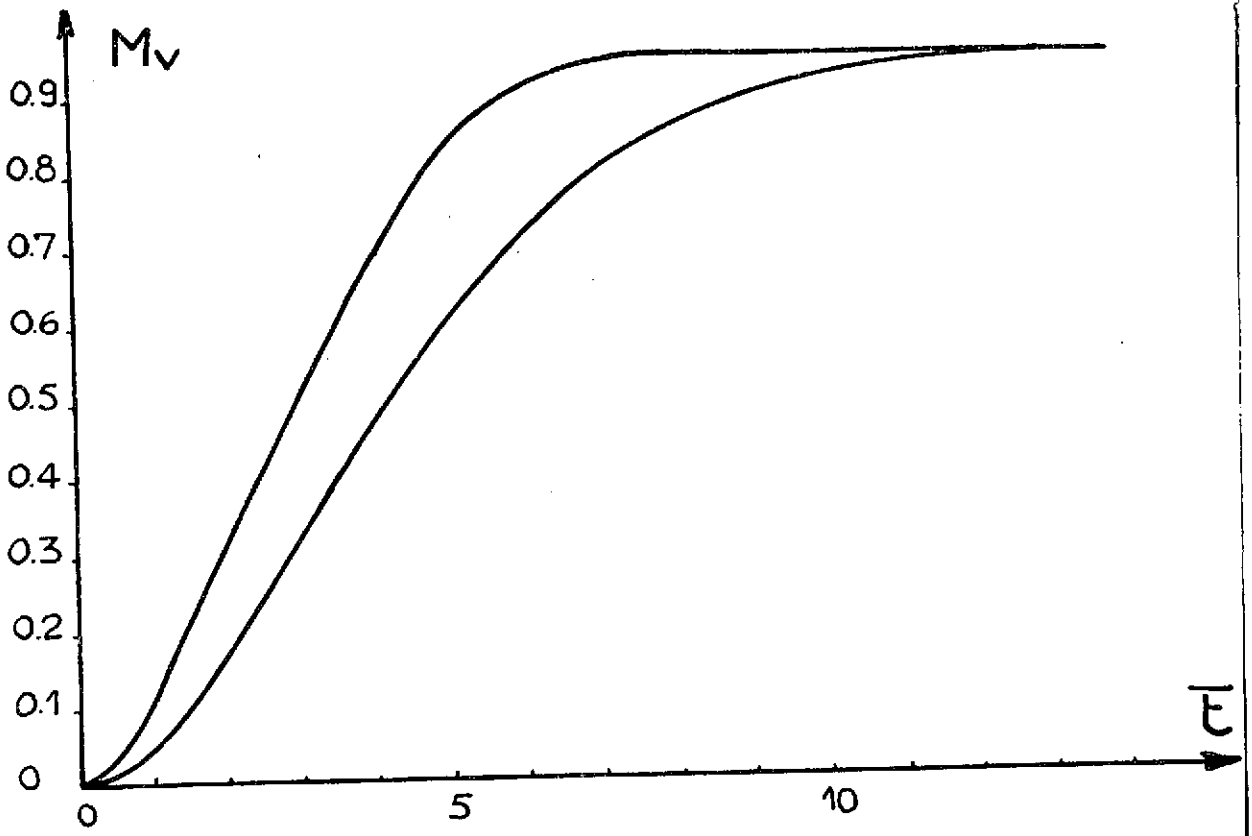

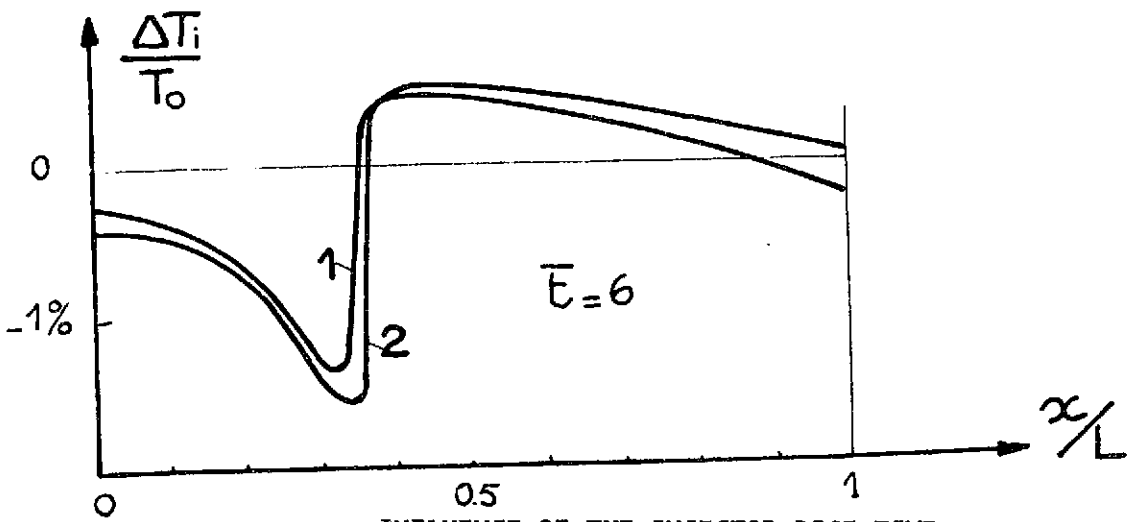

INFLUENCE OF THE INJECTOR RISE TIME

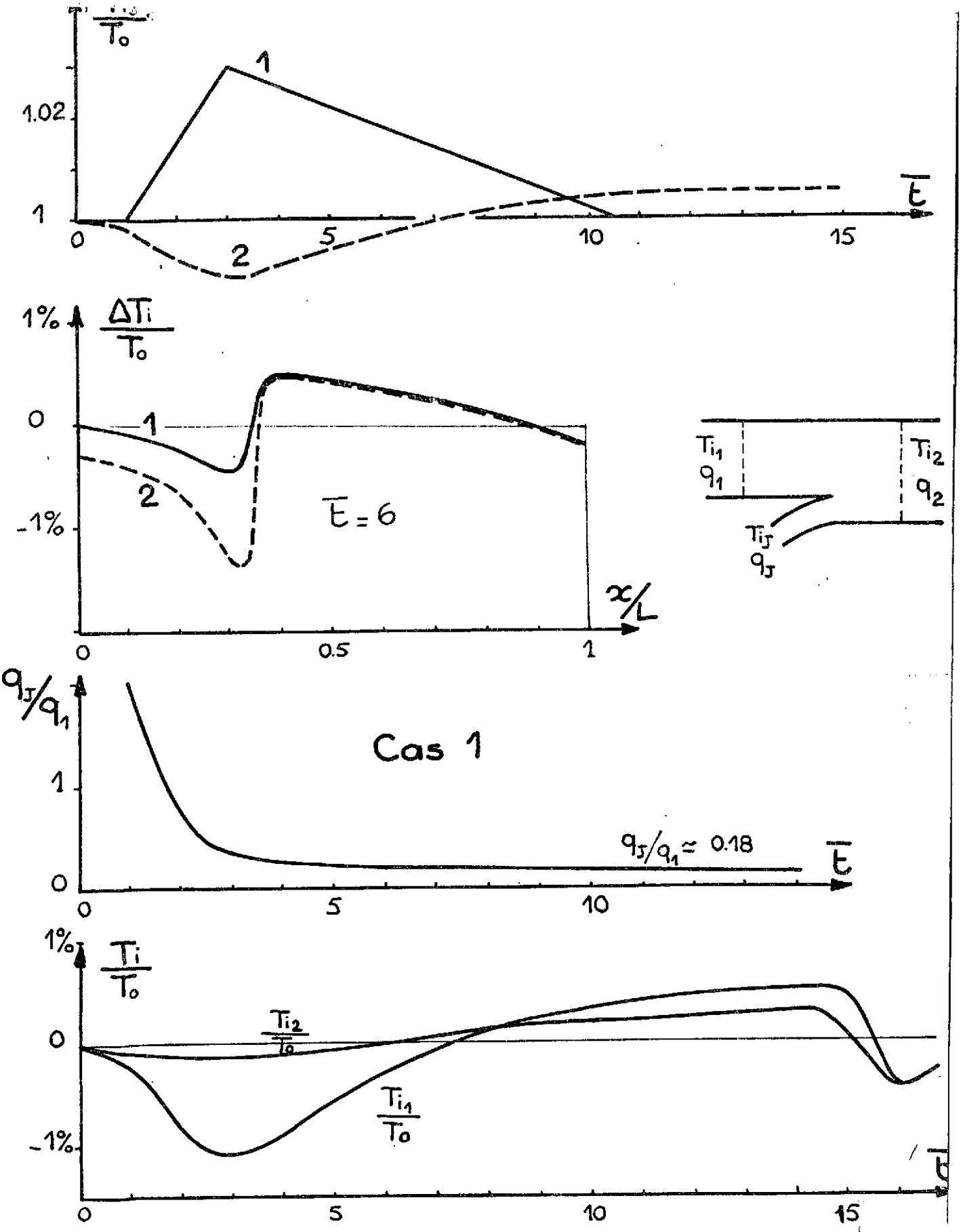
$\frac{T_i}{T_o}$
1.02
1
0
1
2
5
10
15
$\bar{t}$
1%
$\frac{\Delta T_i}{T_o}$
0
-1%
1
2
$\bar{t} = 6$
x/L
0
0.5
1
T_{i_1}
q_1
T_{i_2}
q_2
T_{i_J}
q_J
q_J/q_1
Cas 1
1
0
$q_J/q_1 \simeq 0.18$
$\bar{t}$
0
5
10
1%
$\frac{T_i}{T_o}$
0
-1%
$\frac{T_{i_2}}{T_o}$
$\frac{T_{i_1}}{T_o}$
$\bar{t}$
0
5
10
15